EAST CALIFORNIA 93543-5002

NAVAL POSTGRADUATE SCHOOL
Monterey, California

THESIS

ADAPTIVE MODELING OF THE DYNAMICS

OF AUTONOMOUS LAND VEHICLES

by

James H. Kessler IV

June 1986

Thesis Advisor: Robert B. McGhee

Approved for public release; distribution is unlimited.

T231245

SECURITY CLASSIFICATION OF THIS PAGE

REPORT DOCUMENTATION PAGE

1a. REPORT SECURITY CLASSIFICATION UNCLASSIFIED	1b. RESTRICTIVE MARKINGS
2a. SECURITY CLASSIFICATION AUTHORITY	3. DISTRIBUTION/AVAILABILITY OF REPORT Approved for public release; distribution is unlimited.
2b. DECLASSIFICATION/DOWNGRADING SCHEDULE	
4. PERFORMING ORGANIZATION REPORT NUMBER(S)	5. MONITORING ORGANIZATION REPORT NUMBER(S)
6a. NAME OF PERFORMING ORGANIZATION Naval Postgraduate School	6b. OFFICE SYMBOL (If applicable) 62
6c. ADDRESS (City, State, and ZIP Code) Monterey, California 93943-5100	7a. NAME OF MONITORING ORGANIZATION Naval Postgraduate School
8a. NAME OF FUNDING/SPONSORING ORGANIZATION	8b. OFFICE SYMBOL (If applicable)
8c. ADDRESS (City, State, and ZIP Code)	7b. ADDRESS (City, State, and ZIP Code) Monterey, California 93943-5100
	9. PROCUREMENT INSTRUMENT IDENTIFICATION NUMBER
	10. SOURCE OF FUNDING NUMBERS

PROGRAM ELEMENT NO.	PROJECT NO	TASK NO	WORK UNIT ACCESSION NO

11. TITLE (Include Security Classification)

ADAPTIVE MODELING OF THE DYNAMICS OF AUTONOMOUS LAND VEHICLES

12. PERSONAL AUTHOR(S)
Gessler, James, H

13a. TYPE OF REPORT	13b. TIME COVERED	14. DATE OF REPORT (Year, Month, Day)	15. PAGE COUNT
Engineer's Thesis	FROM _____ TO _____	June 1986	119

16. SUPPLEMENTARY NOTATION

17. COSATI CODES			18. SUBJECT TERMS (Continue on reverse if necessary and identify by block number)
FIELD	GROUP	SUB-GROUP	Parameter identification with unknown inputs, parameter estimation of land vehicles, comparison of identification techniques.

19. ABSTRACT (Continue on reverse if necessary and identify by block number)

This study examines the feasibility of identifying the dynamic parameters of autonomous land vehicles. Initially a simulation study is done using a simplified vehicle model and three different identification schemes. The parameter estimator which has the best characteristics is then used in an improved model to determine if this approach can be used to obtain the parameters of muli-wheeled vehicles.

20. DISTRIBUTION/AVAILABILITY OF ABSTRACT ☒ UNCLASSIFIED/UNLIMITED ☐ SAME AS RPT ☐ DTIC USERS	21. ABSTRACT SECURITY CLASSIFICATION UNCLASSIFIED
22a. NAME OF RESPONSIBLE INDIVIDUAL Prof. Robert B. McGhee	22b. TELEPHONE (Include Area Code) (408) 646- 2095
	22c. OFFICE SYMBOL 52Mz

DD FORM 1473, 84 MAR 83 APR edition may be used until exhausted
All other editions are obsolete

SECURITY CLASSIFICATION OF THIS PAGE

Approved for public release. distribution unlimited.

Adaptive Modeling of the Dynamics of Autonomous Land Vehicles

by

James H. Kessler, IV
Captain. United States Marine Corps
B.S., Rensselaer Polytechnic Institute, 1977

Submitted in partial fulfillment of the
requirements for the degree of

MASTER OF SCIENCE IN ELECTRICAL ENGINEERING
and
ELECTRICAL ENGINEER

from the

NAVAL POSTGRADUATE SCHOOL
June 1986

ABSTRACT

This study examines the feasibility of identifying the dynamic parameters of autonomous land vehicles. Initially a simulation study is done using a simplified vehicle model and three different identification schemes. The parameter estimator which has the best characteristics is then used on an improved model to determine if this approach can be used to obtain the parameters of multi-wheeled vehicles.

TABLE OF CONTENTS

I. INTRODUCTION 7

A. INTRODUCTION 7

B. PROBLEM STATEMENT 7

C. APPROACH 8

D. LIMITATIONS 8

E. STARTING POINT 9

F. ORGANIZATION 9

G. NOTATION 9

II. SURVEY OF PREVIOUS WORK 11

A. INTRODUCTION 11

B. LEAST-SQUARES APPROXIMATION 11

C. KALMAN FILTER IDENTIFIER 16

D. STOCHASTIC GRADIENT ESTIMATION 19

E. SUMMARY 24

III. LEAST-SQUARES IDENTIFIER 26

A. INTRODUCTION 26

B. SIMPLIFIED MODEL FOR SIMULATION STUDY 27

C. INPUT DISTURBANCE AND INITIAL CONDITIONS 31

D. STATE MEASUREMENT NOISE 38

E. STATE DERIVATIVE MEASUREMENT NOISE 38

F. COMBINED NOISE 40

G. COMPUTATIONAL AND STORAGE REQUIREMENTS 43

H. SUMMARY 44

IV. KALMAN FILTER IDENTIFIER 46

A. INTRODUCTION 46

B. INITIALIZATION OF THE KALMAN FILTER 47

C. SYSTEM EXCITATION 51

D. STATE MEASUREMENT NOISE 57

E. STATE DERIVATIVE MEASUREMENT NOISE 65

F. COMBINED NOISE 67

G. INSTRUMENTATION 70

H. COMPUTATIONAL AND STORAGE REQUIREMENTS 71

I. SUMMARY 72

V. STOCHASTIC GRADIENT IDENTIFIER 74

A. INTRODUCTION 74

B. BIAS ELIMINATION 74

C. CHOICE OF THE GAIN MATRIX R(k) 75

D. INITIALIZATION OF R(k) 77

E. SUMMARY 84

VI. IMPROVED MODEL IDENTIFICATION 87

A. INTRODUCTION 87

B. AN IMPROVED MODEL 87

C. IMPROVED VEHICLE PARAMETER IDENTIFICATION 92

1. P(0) Initialization 93

2. Convergence Rate of the Improved Model 95

3. Initial Conditions and Road Noise 97

4. System Identification with Pulse Inputs 99

5. Identification with State Measurement Noise 99

D. TWO INPUTS TO THE IMPROVED MODEL 102

E. COMPUTATIONAL AND STORAGE REQUIREMENTS 106

F. SUMMARY 109

VII. SUMMARY AND CONCLUSIONS 111

A. INTRODUCTION 111

B. RESULTS 111

C. FURTHER STUDY 114

LIST OF REFERENCES 116

I. INTRODUCTION

A. INTRODUCTION

In recent years the concept of autonomous vehicles has become a reality. Martin Marietta Corp. has built an autonomous wheeled vehicle [Ref. 1]. FMC Corporation is developing a tracked autonomous vehicle [Ref. 2]. Ohio State University is constructing a six legged vehicle [Ref. 3].

As autonomous vehicles progress it will become necessary for them to identify their own dynamic parameters in order to operate effectively. This will allow the vehicle to identify its mass and other characteristics and determine if it can operate within the envelope for which it was designed. This would also enable the vehicle to continuously monitor its parameters and identify maintenance problems or other potential problems and take the necessary steps to prevent damage to itself. This capability would give the vehicle what all natural autonomous systems have, the ability to "feel" their own dynamic parameters.

B. PROBLEM STATEMENT

The objective of this thesis is to determine the feasibility of using parameter identification techniques to identify the dynamic parameters of an autonomous vehicle, on line, and to monitor variations in those parameters during operation. The term on-line in this case means, while operating normally. The desire here is

to allow the vehicle to passively identify its parameters without the need to actively participate in developing inputs specifically selected for identification.

In this thesis, continuous time parameters will be identified. This will increase the hardware requirements, but will allow for certain other desirable features required for multi-wheeled vehicles. Thus, the problem of this thesis is to passively identify and track the continuous time dynamic parameters of a wheeled vehicle.

C. APPROACH

The number of different parameter identification techniques available is extensive, but many of the approaches are similar. Two major distinction are, the ability to identify nonlinear systems, and to allow stochastic inputs. The work of this thesis is directed toward problems solvable by stochastic linear identifiers. Here, three approaches will be considered in detail. First each technique will be presented mathematically and then used in a simulation study to analyze their respective characteristics. A simplified vehicle model will be used for this purpose. The scheme found to have the most desirable properties will then be used to identify the parameters of a more realistic model. This will determine if the approach is valid for the identification of wheeled vehicles. From these results, the feasibility of identifying and tracking the vehicle parameters will be considered.

D. LIMITATIONS

In the development of a simulation study some assumptions must necessarily be made. In this thesis, it will be assumed that the input from the road is white noise. In addition, it will be assumed that position, velocity, and acceleration are available for the vehicle's body and all of its wheels.

E. STARTING POINT

The field of parameter identification is well developed. The standard approach to parameter estimation is with respect to scalar discrete time systems. In this analysis a multi-input multi-output continuous-time parameter identifier is used. This will require certain changes to the standard algorithms used in the literature.

F. ORGANIZATION

The mathematical development of the three identification schemes will be presented in the next chapter. In the following three chapters, each approach will be analyzed using a simulation study on a simplified model that is presented in Chapter III. In Chapter VI, the technique which demonstrated the best characteristic during the simulation study will be used on an improved model developed in that chapter. Chapter VII will present the concluding remarks concerning the feasibility of this from of parameter identification when used on land vehicles.

implies large initial excitation which would have the added quality of producing a rapidly decreasing $P(k)$ matrix causing c in Equation 4.17 to be small.

Figure 4-5 shows this cumulative bias quite clearly, for three different values of measurement noise. Notice the two lower curves marked by triangles and "+" symbols, which show the error measurement ξ_k for σ_w equal to 1 % of the standard deviation of the road noise, and no state measurement noise, respectively. These curves indicate that for small values of σ_w the identification process is only slightly biased, but even for this small value of measurement noise there is a cumulative bias. However, if σ_w is 2% of the standard deviation of the input road noise, the identification is seriously impeded, as shown by the curve marked with circles. The curve marked with squares is for σ_w equal to 4 % of σ_u, and it is clear that in 10000 iterations no improvement has been made in the normalized estimation error ξ_k. In fact for values of σ_w larger than 2 % of σ_u, the parameter estimation is divergent.

Figure 4-6 is an illustration of the bias accumulated over 40,000 iterations when σ_w is 2 % of σ_u. Figure 4-6 should be compared with Figure 4-2, where after 40,000 iterations the difference between the two error measures ξ_k is about 1.

Since the affect of σ_w is so profound on the estimation process, it seems appropriate to obtain a signal to noise ratio for the state vector which will achieve acceptable results. Recall that the standard deviation of the output of a linear system is given by [Ref. 8:p. 184]

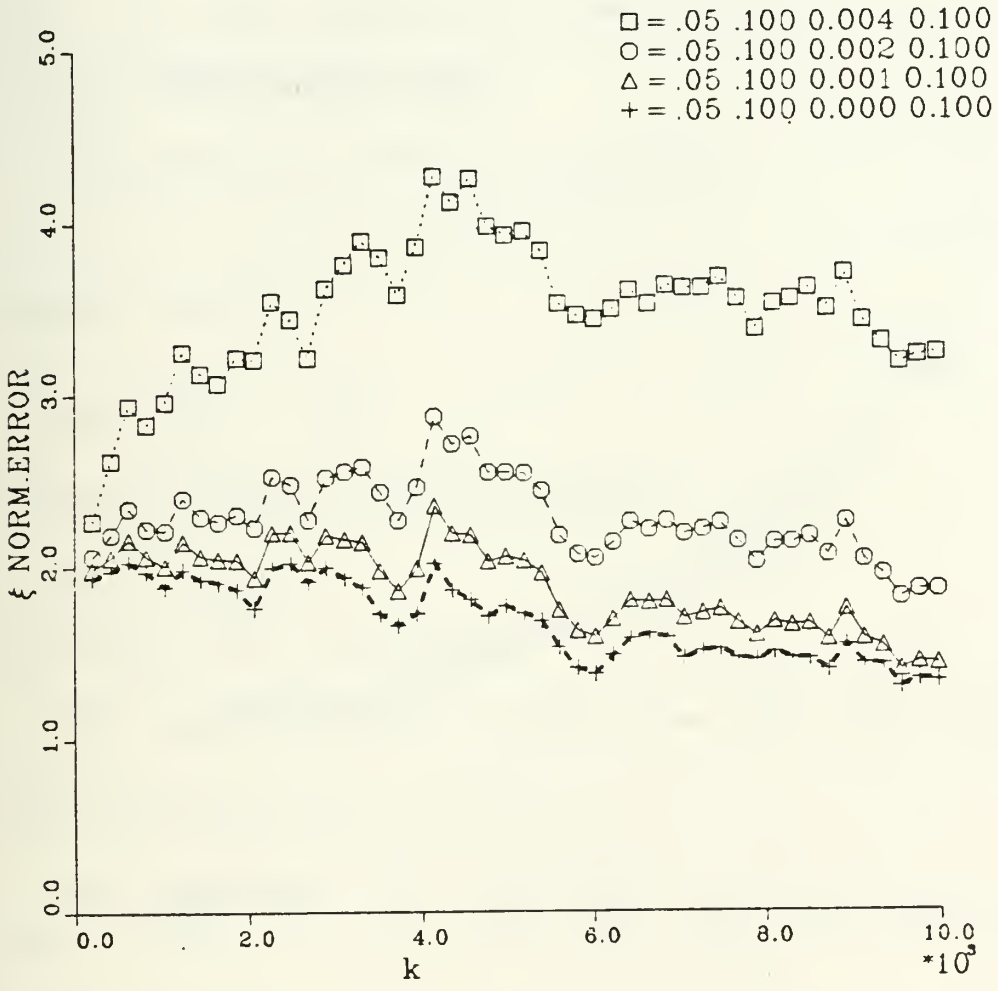

Figure 4-5 Parameter estimation vs. number of iterations with road noise as excitation and various level of state measurement noise.
Initial conditions, σ =0.05
Road noise, σ =0.1
State measurement noise, σ =0.004, 0.002, 0.001, 0.0005
State derivative measurement noise, σ =0.1.

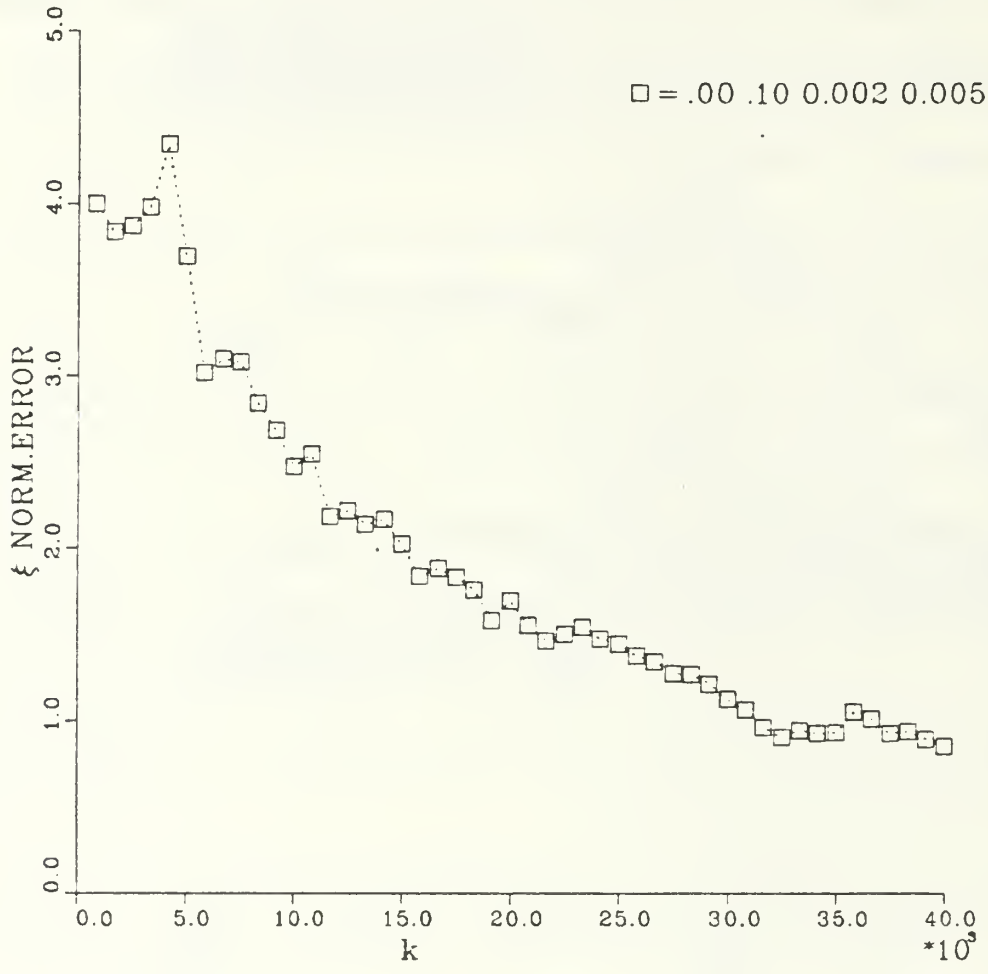

Figure 4-6 Parameter estimation vs. number of iterations with road noise as the only system excitation.
Initial conditions, σ =0.0
Road noise, σ =0.1
State measurement noise, σ =0.002
State derivative measurement noise, σ =0.005.

$$\sigma^2_{out} = \frac{1}{\pi}\int_0^{\infty} |H(\omega)|^2 S_u(\omega)\, d\omega \tag{4.18}$$

where $|H(\omega)|$ is the magnitude of the transfer function and $S_u(\omega)$ is the power spectral density of the input signal.

The transfer function H(s) can be obtained from

$$X(s) = (sI-A)^{-1}x(0) + (sI-A)^{-1}BU(s) \tag{4.19}$$

or if x(0) is zero. then

$$H(s) = \frac{X(s)}{U(s)} = (sI-A)^{-1}B \tag{4.20}$$

The magnitude squared of $H(s)$ is derived from

$$|H(s)|^2 = H(s)H(-s) \tag{4.21}$$

and replacing s by jw produces $|H(w)|^2$.

The system is excited by a discrete noise source whose autocorrelation function can easily be derived. Since

$$R_u(\tau) = E[u(t)u(t-\tau)] \tag{4.22}$$

then

$$R_u(0) = E[u^2] = \sigma_u^2 \tag{4.23}$$

and

$$R_u(\tau) = 0 \quad \text{for} \quad |\tau| > T \tag{4.24}$$

so that

$$R_u(\tau) = \begin{cases} \sigma_u^2\left[1 - \dfrac{|\tau|}{T}\right] & ,|\tau| \le T \\ 0 & ,|\tau| > T \end{cases} \tag{4.25}$$

where T is the pulse width of the discrete noise source [Ref. 8:p. 121]. Figure 4-7

depicts the autocorrelation function of the discrete road noise. The power spectral density of this process is. [Ref. 8:App. E]

$$S_u(\omega) = \sigma_u^2 \left[T \frac{\sin^2(\omega T/2)}{(\omega T/2)^2} \right] \tag{4.26}$$

Therefore, the standard deviation of the output is

$$\sigma_i^2 = \frac{T\sigma_u^2}{\pi} \int_0^\infty |H_i(\omega)|^2 \left[\frac{\sin(\omega T/2)}{(\omega T/2)} \right]^2 d\omega \tag{4.27}$$

where i denotes the associated state variable $i = 1,2,3,4$. Using numerical integration. the output standard deviations σ_z of the state vector are

$$\sigma_z = \begin{bmatrix} .386 \\ 1.84 \\ .402 \\ 1.03 \end{bmatrix} \sigma_u \tag{4.28}$$

The observed standard deviations of the state vector during simulation of the simplified model for four different ensembles of road noise and average over 10000 measurements are as follows:

$$\frac{\sigma_z}{\sigma_u} = \begin{bmatrix} .366 \\ 1.78 \\ .368 \\ .941 \end{bmatrix}, \begin{bmatrix} .390 \\ 1.83 \\ .403 \\ 1.05 \end{bmatrix}, \begin{bmatrix} .352 \\ 1.76 \\ .372 \\ .922 \end{bmatrix}, \begin{bmatrix} .372 \\ 1.80 \\ .388 \\ 1.03 \end{bmatrix} \tag{4.29}$$

These results are in excellent agreement with the analytic results of Equation 4.28 . Some interesting observations can be made from these results. Note that for a given level of road noise σ_u, the wheel velocities σ_{x_2} are almost twice as large as the input noise values. Written in equation form this becomes

$$\sigma_{z_2} = 1.84\sigma_u \tag{4.30}$$

The vehicle body velocities reflect the input noise almost exactly. Also, the

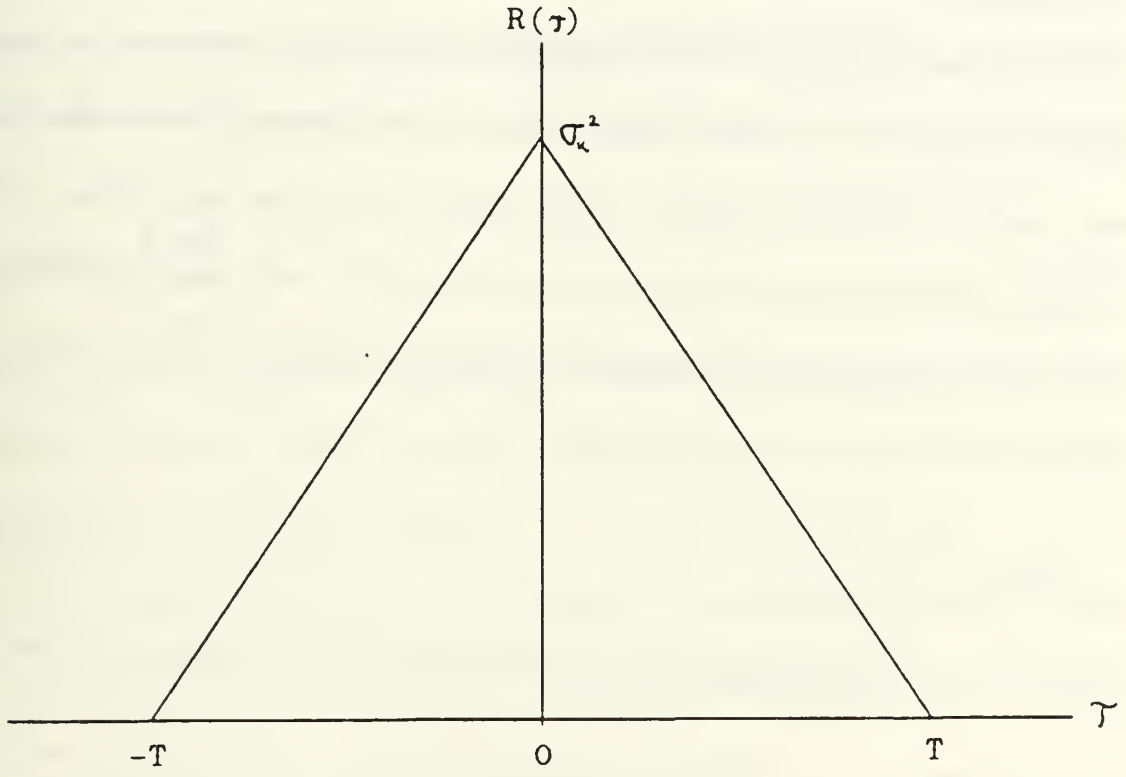

Figure 4-7 Autocorrelation function for discrete road noise with T =0.05

position change of the wheels and the body attenuates the input road noise significantly.

The results in Equation 4.28, give the standard deviation of the state vector with only road noise as input to the simplified vehicle. Evidently, if measurement noise is applied uniformly to the component measurements of the state, some of them will suffer more corruption than others. In order to dissect the identification error caused by the noise added to each element of the state vector when σ_w is uniformly applied to each element, the noise was added to only one element of the state vector at a time during simulation. The signal to noise ratio at each sensor is given by

$$\frac{S_i}{N} = \eta_i = \frac{\sigma_i}{\sigma_w} = \frac{\sigma_i}{\sigma_u}\frac{\sigma_u}{\sigma_w} \tag{4.31}$$

where the i denotes the element of the state vector and $\frac{\sigma_i}{\sigma_u}$ is given in Equation 4.28 . Therefore, if the road noise standard deviation σ_u is 25 times greater than the state measurement noise standard deviation σ_w, then the signal to noise ratio at each sensor is

$$\frac{S_i}{N} = \begin{bmatrix} .386 \\ 1.84 \\ .402 \\ 1.03 \end{bmatrix} 25 = \begin{bmatrix} 9.65 \\ 46.0 \\ 10.0 \\ 25.8 \end{bmatrix} = \begin{bmatrix} 19.7 \\ 33.3 \\ 20.0 \\ 28.2 \end{bmatrix} dB. \tag{4.32}$$

Define $e_i(k)$ as

$$e_i(k) = \xi_{w_i}(k) - \xi_0(k) \tag{4.33}$$

where $\xi_{w_i}(k)$ is the error measure with state measurement noise added to only the

ith element of the state vector and $\xi_0(k)$ is the error measure after k iterations without any state measurement noise applied.

By adding state measurement noise to only one element of the state vector at a time, the effect of the added noise on each element can be seen. Three simulations were run, each with a different ensemble of noise and the average error caused by adding measurement noise to each element of the state vector was

$$e_i(8000) = \begin{bmatrix} .605 \\ .001 \\ .705 \\ .032 \end{bmatrix} \tag{4.34}$$

Notice here that the sensor with a 33.3 dB signal to noise ratio produces only a very small bias error at 8000 iterations, while the sensor with a sensitivity of 28.2 dB. produces a bias 30 times as large.

More analysis could be done on this topic, but it is sufficient to conclude that the necessary signal to noise ratio for each sensor is about 33 dB.

E. STATE DERIVATIVE MEASUREMENT NOISE

The Kalman filter identifier can identify the parameters of the simplified vehicle through the state derivative noise introduced by the random vector $v(k)$. Since this algorithm is a weighted least squares method, and is recursive, the size of σ_v determines only the length of time required to identify the parameters. The accuracy of the estimates can be arbitrarily close to the actual values given the appropriate number of iterations.

However, should the standard deviation of the vector $v(t)$ be underestimated the result will be a biased estimate of the parameters. Because the $P(k)$ matrix diminishes too rapidly, the parameters cannot be estimated before the gain matrix becomes very small and no significant change in the parameter estimates can be expected. This bias leads to a very serious limitation of the Kalman filter identifier, which requires either extended observation time or acceptance of a bias produced by the excess road noise. The long observation time is required since the standard deviation of the road noise must be estimated large to allow for large road noise inputs, which in turn will cause very slow convergence.

The need to eliminate this excess excitation bias points to a reinitialization scheme, which will restart the gain matrix and allow identification to continue. This scheme is used whenever the filters perceived error in the error covariance matrix becomes exceedingly small, while the actual measured error given by

$$e(k) = z - H\hat{\theta} = [\, e_1, \ldots, e_n(k) \,]^T \tag{4.35}$$

remains relatively large. The reinitialization of the identifier will eliminate this form of bias, but will not improve the required estimation time directly. The advantage of choosing the R matrix smaller than the actual value of the noise covariance is obvious from Figure 4-8. What is less obvious is exactly how to determine when to reinitialize and how much to increase the diagonal of the P matrix. Figure 4-8 demonstrates the effectiveness of a reinitialization procedure that multiplies the diagonal elements of the P matrix by ten and doubles the elements of the R matrix when the sum of the diagonal elements of the P matrix

become smaller than ten times the sum of the error vector in Equation 4.35 . This scheme is given in equation form as

$$10\sum_{i=1}^{n} |e_i(k)| > \sum_{j=1}^{n^2} P_{jj}(k) \qquad (4.36)$$

Figure 4-8 illustrates the advantage of a reinitialization procedure. The curve marked with squares was produced using an identifier with the correct values in the noise covariance matrix R. The other three curves denote identifiers which initially had smaller values in the R matrix, as shown in the legend. The reinitialization scheme is visible at several point along the curve marked by "+" symbols. The most obvious reinitialization happens at about 5000 iterations, when both the curve marked by triangles and the one marked with "+" symbols are reinitialized. It seems evident that reinitialization can be applied whenever the state derivative noise is larger than anticipated, or very little is known about the noise source, as in the case of road noise.

F. COMBINED NOISE

The combination of all the noise sources results in essentially the same identification performance as would be expected from the worst individual source, just as it did for the least squares approach of Chapter III. Figure 4-9 shows that the effect of state derivative measurement noise is insignificant when compared with the effect of even very small values of state measurement noise. The correlation of the $H(k)$ matrix and the input noise $v(k)$ as described in Equation 2.20 is the cause of the bias due to state measurement noise. In the case where

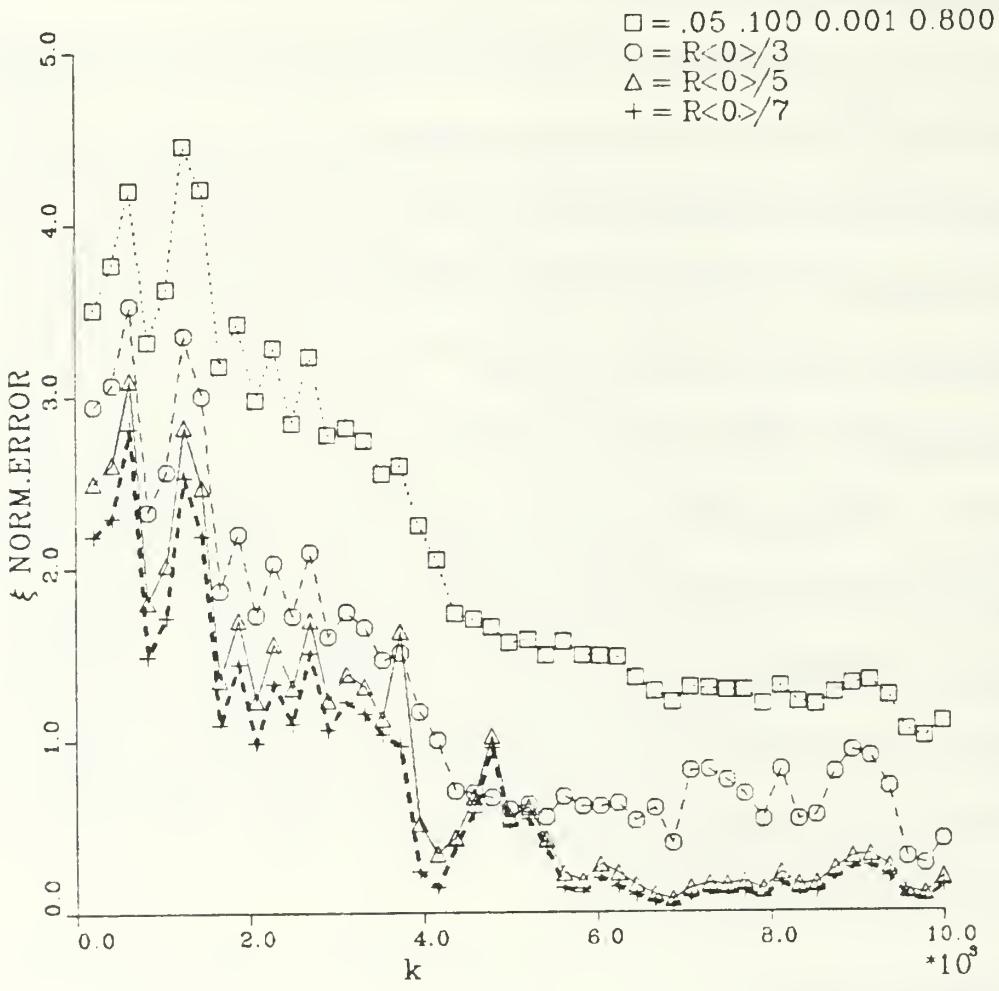

Figure 4-8 Parameter estimation vs. number of iterations with incorrect selections of the road noise covariance matrix using reinitialization to continue the identification process.
Initial conditions, σ =0.05
Road noise, σ =0.1
State measurement noise, σ =0.001
State derivative measurement noise, σ =0.8.

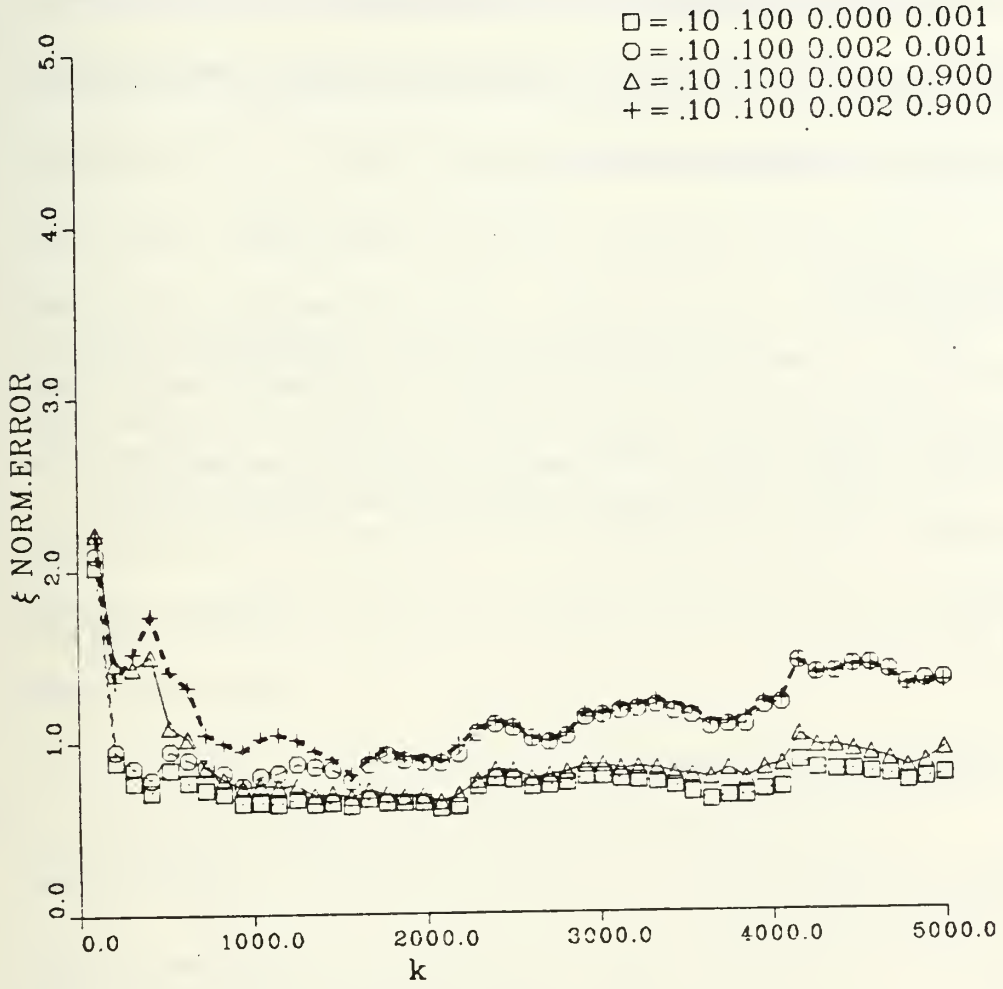

Figure 4-9 Parameter estimation vs. number of iterations for various levels of statemeasurement noise and state derivative measurement noise.
Initial conditions, σ =0.1
Road noise, σ =0.1
State measurement noise, σ =0.000, 0.002, 0.000, 0.002
State derivative measurement noise, σ =0.001, 0.001, 0.900, 0.900.

only σ_t was applied, as in the curve marked by triangles, it has very little effect on the identifier. When state measurement noise is present however, the error introduced is quite significant. When both noise sources are applied the outcome is equivalent to only state measurement noise.

G. INSTRUMENTATION

In Chapter III it was assumed that the state vector measurement and the state derivative vector measurement were obtained from separate instruments. In this chapter, a more realistic instrumentation philosophy was employed. Since

$$\begin{pmatrix} \dot{x}_1 \\ \dot{x}_3 \end{pmatrix} = \begin{pmatrix} x_2 \\ x_4 \end{pmatrix} \tag{4.37}$$

then the noisy measurements are given by

$$\begin{pmatrix} z_1 \\ z_3 \end{pmatrix} = \begin{pmatrix} \dot{x}_1 + v_1 \\ \dot{x}_3 + v_3 \end{pmatrix} = \begin{pmatrix} x_2 + w_2 \\ x_4 + w_4 \end{pmatrix} = \begin{pmatrix} r_2 \\ r_4 \end{pmatrix} \tag{4.38}$$

Thus, when only one measurement is taken of each physically distinct component of the state vector, it follows that

$$\begin{pmatrix} v_1 \\ v_3 \end{pmatrix} = \begin{pmatrix} w_2 \\ w_4 \end{pmatrix} \tag{4.39}$$

This does not significantly affect the results of Chapter III, for the reasons given in the summary of that chapter, but it does reduce the number of measurements of the system from 8 to 6.

The measurements taken on each mass are the acceleration $\ddot{x}$, the velocity $\dot{x}$, and the position x. While the acceleration measure can be allowed to be noisy, the velocity and the position must have a signal to noise ratio of 33 dB. The acceleration will no doubt be obtained from an accelerometer, but the velocity and position measurements could be obtained in a variety of ways. Since integration is inherently a noise reducing process, it should be possible to integrate the acceleration to obtain the velocity and integrate the velocity to obtain the position. This could be done with analog or digital techniques and the choice might very well depend on the computational load on the microprocessor used in the identifier. Some drift correction would of course be required over long measurement times.

H. COMPUTATIONAL AND STORAGE REQUIREMENTS

The Kalman filter identifier places a large burden on the microcomputer during its operation. Table I presents a rough calculation of the typical cycle time for the 4 state, 6 measurement Kalman filter examined in this chapter. Adding up the times in the bottom row of this table gives a total cycle time of 3622 μ seconds. While the numbers used for the time required for each operation are somewhat arbitrary, they are typical, and thus it seems quite possible to process a measurement every 0.05 seconds, as was done in the simulations of this chapter. The storage requirement for this algorithm was 352 bytes of memory. This is a

Table I. Cycle time for the Kalman filter identifier

to compute	operation				
	mult	divid	add	inc/load	store
G=PH[HPH+R]	80	2	56	158/104	30
P=[I-GH]P	160	0	104	160/152	104
x=x+Ge	16	0	18	35/ 46	18
total ops	256	2	178	353/302	152
time/op (μsec)	6	8	2	2	2
total time	1536	16	356	1310	304

considerable improvement over the least squares identifier requirement of 1 Megabyte.

It is quite possible that this identifier could be implemented on a very small circuit board with only the microprocessor. a 1 kilobyte ROM chip. 512 bytes of static ram and 6 buffer chips to receive the discrete state and state derivative measurements.

I. SUMMARY

The Kalman filter identifier has several advantages over the least squares approach, with very few disadvantages. Because the Kalman filter is a recursive weighted least squares algorithm, it requires less memory. More importantly, since this approach is a Kalman filter, it provides an organized and meaningful way of choosing the weightings and the initial conditions. The identifier is capable of finding the parameters even when considerable road noise and state derivative measurement noise are present. This approach is not capable of producing an unbiased estimate of the parameters in the presents of state measurement noise. The signal to noise ratio of the sensors must be better than 33 dB in order to produce an unbiased estimate of the parameters. This signal to noise ratio is fairly close to the one found in Chapter III, using a very simple approach. The requirement for near perfect state measurement is a limitation of both the least squares and Kalman filter approachs. This limitation, though constraining, is not unacceptable, due to the recent advances in accelerometers and ring laser gyros. It will make the use of expensive hardware a necessity, however. In the next chapter, the stochastic gradient approach is evaluated. The stochastic gradient approach promises to remove the need for perfect state measurement and still produce an unbiased estimate.

V. STOCHASTIC GRADIENT IDENTIFIER

A. INTRODUCTION

The stochastic gradient identifier is perhaps the simplest algorithm that can be applied for parameter identification. This simplicity has the price of slower convergence. In this chapter the stochastic gradient approach will be analyzed using a simulation study and the same simple vehicle model as in the last two chapters. This algorithm promises to eliminate the need for perfect state measurements which is a very desirable feature.

Recall from Chapter II, that for the system defined by

$$z(k) = H_r(k)\theta + v(k) \tag{5.1}$$

where $v(k)$ represents both disturbance and measurement noise, and $H_r(k)$ is defined in Equation 2.19, that the stochastic gradient algorithm is

$$\hat{\theta}(k+1) = [I + R(k)\Sigma_N]\hat{\theta}(k) + R(k)H_r^T(k)\tilde{z}(k) - R(k)E[H^T(k)v(k)] \tag{5.2}$$

This equation was derived under the assumption that all three noise sources used in Chapters II and III would be present, and therefore the algorithm will produce an unbiased estimate of the parameters of the vehicle in the presence of: $u(t)$ the road noise, $w(t)$ the state measurement noise, and $v(t)$ the state derivative measurement noise.

B. BIAS ELIMINATION

If Equation 5.2 is broken up into components associated with either parameter identification or bias elimination the result is

$$\hat{\theta}(k+1) = \hat{\theta}(k) + R(k)H_r^T(k)\tilde{z}(k) \tag{5.3}$$

$$+ R(k)\Sigma_N\hat{\theta}(k) - R(k)E[H^T(k)v(k)]$$

The two elements on the second line of Equation 5.3 are used to reduce the bias: the first uses Σ_N, the covariance matrix of the state measurement noise N(k), and the second uses the input-output cross correlation $E[H^T(k)v(k)]$.

The value of the state measurement noise covariance matrix, Σ_N is easily obtained from

$$\Sigma_N = E[N^T(k)N(k)] \tag{5.4}$$

which is a block diagonal matrix, with n blocks of $n \times n$ elements equal to σ_w^2.

The value of the input-output crosscorrelation matrix is somewhat more difficult to obtain, but in this simplified model with a single input which is white noise the crosscorrelation is

$$E[H^T(k)v(k)] = E[H^T(k)]\ E[v(k)] = 0 \tag{5.5}$$

because $v(k)$ is assumed to be zero mean. This simplification leads to the algorithm

$$\hat{\theta}(k+1) = [I + R(k)\Sigma_N]\hat{\theta}(k) - R(k)H_r^T(k)\tilde{z}(k) \tag{5.6}$$

where the determination of $R(k)$ is the subject of the next section.

C. CHOICE OF THE GAIN MATRIX R(k)

There are many possible choices for the gain matrix R(k), only two of which were introduced in Chapter II. The R(k) matrices discussed in Chapter II were chosen because of their computational simplicity. However, another requirement is that R(k) must be independent of H(k) and $\hat{\theta}(k)$, which was a requirement for the derivation of Equation 5.2 . Two rather substantial problems become apparent immediately: first the need to make $H(k+l)$ and $H(k)$ statistically independent, and second the slow convergence of the algorithm due to the simple steepest descent gain matrix chosen as R(k). In order to make $H(k+l)$ and $H(k)$ independent in this simplified vehicle they must be separated in time by four time constants of the system or 5.6 seconds. This separation means that very extended observation times will be needed to reach an acceptable parameter approximation. The simple selection of the gain matrix R(k), which at first glance may seem to be a computational advantage, will require more iterations to obtain acceptable results than many of its more sophisticated counterparts.

One final observation can be made concerning the stability of Equations 5.2 and 5.6 , before proceeding into the simulation study. Consider again Equation 5.6 in the dynamic systems sense and notice the time varying state transition matrix given as

$$\Phi(k) = |I + R(k)\Sigma_N \tag{5.7}$$

For this discrete time system, the characteristic equation will certainly have poles on the unit circle, and if state measurement noise is present then the roots will all

be outside the unit circle, since both $R(k)$, the gain matrix and Σ_N, the state measurement noise covariance matrix are positive definite. It seem reasonable that the magnitude of $R(k)$ and its rate of decay will play a very important role in determining whether successful identification is made. However, there is very little information available concerning how to select an optimal $R(k)$ matrix. Thus the first part of the simulation study is devoted to the proper selection of $R(k)$.

D. INITIALIZATION OF R(k)

In Chapter II, two choices for the gain matrix $R(k)$ were presented. The first based on Venter's theorem was

$$R(k) = \frac{1}{k^p} diag[h_1(k), h_2(k), \ldots, h_{n^2}] \qquad \text{for } \frac{1}{2} < p \leq 1 \tag{5.8}$$

and the second based on Lyapunov's Main Stability theorem was

$$R(k) = \frac{diag[h_1(k), h_2(k), \ldots, h_{n^2}]}{\sum_{i=1}^{n^2} h_i(k) r_i^2(k)} \tag{5.9}$$

where $h_i(k)$ can vary for different anticipated values of θ. The second gain matrix, in Equation 5.9 is not independent of H(k) and although Mendel [Ref. 4:p. 268] suggests its use, it will probably result in a biased estimate.

Figure 5-1 shows the difference in convergence, when the two different choices of $R(k)$ are used in the absence of measurement noise while the system is excited by road noise. Again, the error measure ξ_k is used to determine how close the parameters estimates are to the actual parameters. The curve marked with

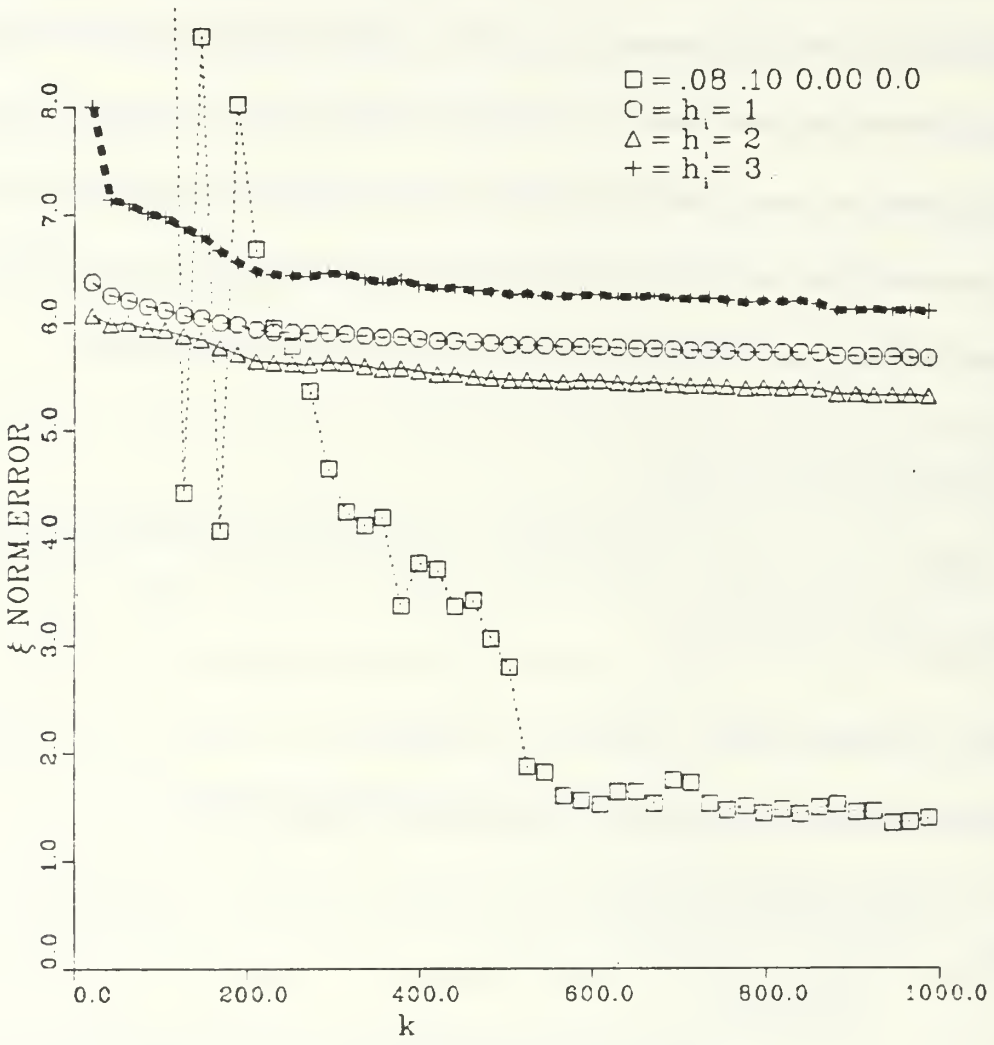

Figure 5-1 Parameter estimation error for Lyapunov gain matrix and three different values of diagonal elements for Venters gain matrix.
Initial conditions, $\sigma = 0.08$
Road noise, $\sigma = 0.1$
State measurement noise, $\sigma = 0.0$
State derivative measurement noise, $\sigma = 0.0$

squares is the error measure ξ_k when $R(k)$ is chosen as in Equation 5.9, while the other three curves are for various values of $h_i(k)$ using Equation 5.8 to determine $R(k)$, while holding p constant at 0.51. The curve derived from the use of Equation 5.9 initially reaches the smallest value and then stablizes as do the other three curves. This is due to the more responsive nature of Equation 5.9 and the larger variations in the bottom curve when compared with the upper three curves also demonstrates this. The error measure marked by circles has the smallest elements in the R(k) matrix and is therefore the least responsive as can be seen in the figure. The curve marked with "+" symbols has larger elements in the R(k) matrix and represents the largest elements that can be expected to produce acceptable convergence. The curve marked with triangles performs the best with smaller elements of R(k), and will produce more consistent results, particularly in the presents of noise. For this simulation, the separation time between measurements was 0.05 seconds, thus for the 1000 iterations represented here the total observation time is about 50 seconds. This time period has produced results which are worse than the Kalman filter approach normally produces in the first 5.0 seconds of it's operation, when starting with the same initial conditions.

This slow convergence in the absence of noise is quite troublesome. In fact if the identifiers convergence rate remained constant, which it certainly will not since convergence is asymptotic, it would still require approximately 18 hours to reach an acceptable approximation in the presence of measurement noise. There

are few identification scenarios in which 18 hours is considered appropriate for system identification. If the system is initially known and one was attempting to follow time varying parameters this approach might be more appealing.

The road noise in the vehicle model produced very large deviations from the actual second row parameters if the $h_i(k)$ values for that row became too large. The identifier produced the best results when

$$10h_i(k) = h_{i+4}(k) \qquad \text{for } i=1,2,3,4 \tag{5.10}$$

Figure 5-2 shows the error measurement curve for the same noise ensemble as used in Figure 5-1 but with state measurement noise added. Comparing the effect of the added noise on the Venter gain matrix $R_v(k)$ and the Lyapunov gain matrix $R_l(k)$, it can easily be seen that $R_l(k)$ is profoundly effected while the curve resulting from the use of $R_v(k)$ is nearly unchanged. This change in the error measurement curve due to the use of $R_l(k)$ is the result of the correlation of $R_l(k)$ and $H(k)$ which were assumed uncorrelated in Equation 2.57 . Therefore, the use of $R_l(k)$ will produce a bias and the use of $R_v(k)$ produces extended observation time. Since the stochastic gradient approach was chosen because it promised to produce an unbiased approximation of the parameters, the gain matrix $R_l(k)$ will not be explored further.

The slow convergence rate of the steepest descent stochastic gradient identifier must be improved in order to make the identification scheme acceptable. There are several factors which affect the convergence rate which can be explored in an attempt to improve the convergence. In Figures 5-1 and 5-2, the value of p

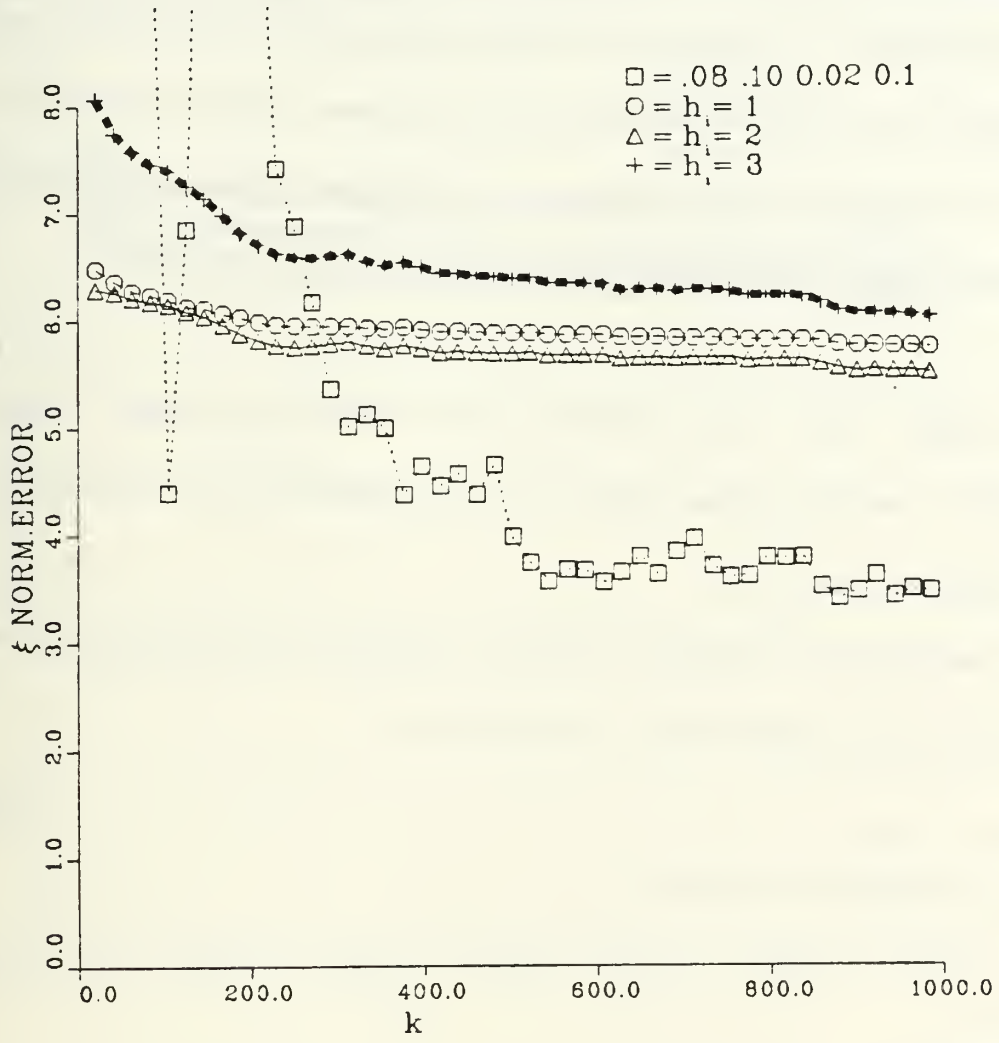

Figure 5-2 Parameter estimation error for Lyapunov gain matrix and three different values of diagonal elements for Venters gain matrix.
Initial conditions. $\sigma = 0.08$
Road noise. $\sigma = 0.1$
State measurement noise. $\sigma = 0.02$
State derivative measurement noise. $\sigma = 0.1$

the power to which k is raised in Equation 5.8, was 0.51. Figure 5-3 demonstrates the effect changing p to 0.95 has on the error measurement in the presence of measurement noise. Since p is now larger, which will force $R(k)$ to diminish more rapidly, one might have expected that the use of larger values of $h_1(k)$ would produce better results. This was not the case, and

$$h_1(k)=4 \tag{5.11}$$

was the largest value that converged in the presence of noise. Without measurement noise much larger values of $h_1(k)$ are possible, but the convergence rate is only slightly improved.

It is possible that the optimum value for p is between 0.51 and 0.95. However, Ljung [Ref. 6:p. 279] suggests that it is desirable to let

$$t\gamma(t)\rightarrow 1 \quad \text{as} \quad t\rightarrow\infty \tag{5.12}$$

where $\gamma(t)$ is defined in this thesis as

$$\gamma(k) = \frac{1}{k^p} \tag{5.13}$$

This implies that

$$\gamma(k) = \frac{1}{k} \tag{5.14}$$

It is also suggested that for small and intermediate values of k, $\gamma(k)$ should be chosen differently. Thus define

$$\gamma(k) = \frac{1}{1+\dfrac{\lambda(k)}{\gamma(k-1)}} \tag{5.15}$$

and

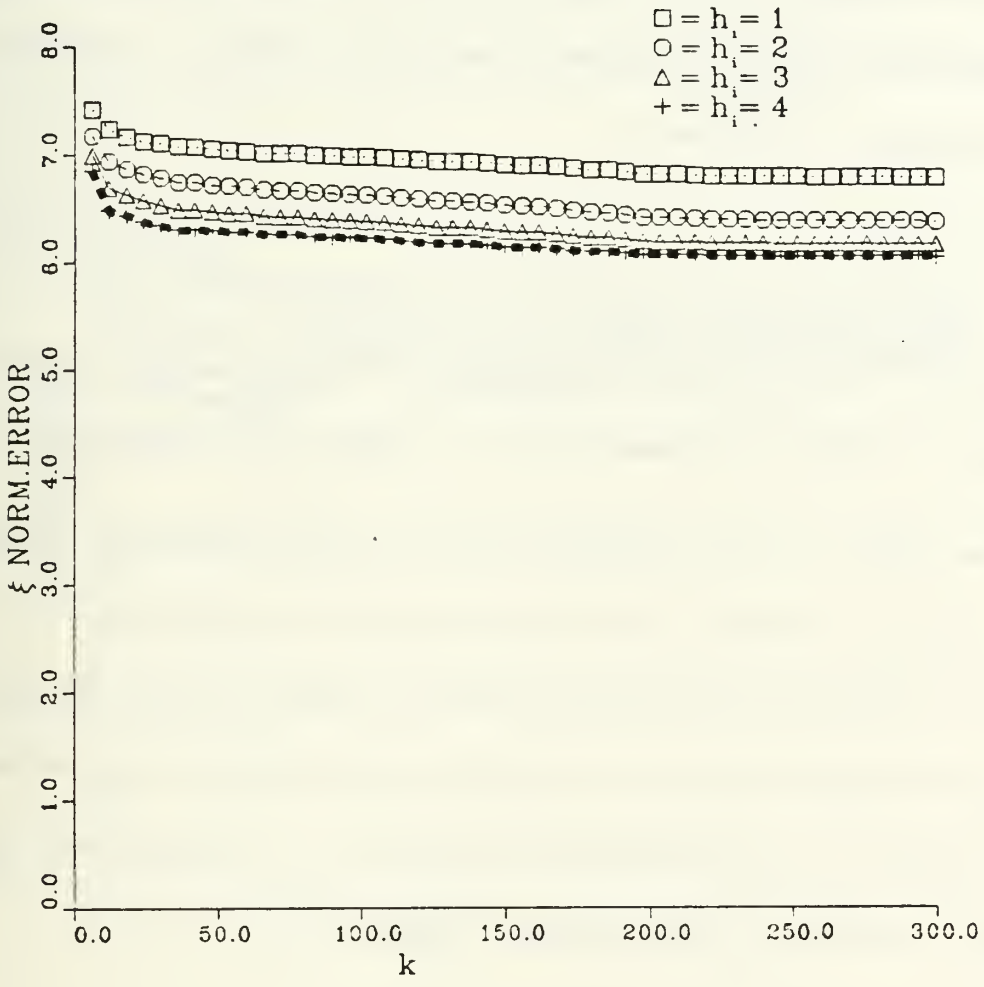

Figure 5-3 Parameter estimation error for four
different values of diagonal elements for Venters gain matrix.
and p=0.95.
Initial conditions. σ = 0.08
Road noise, σ = 0.1
State measurement noise, σ = 0.02
State derivative measurement noise, σ = 0.1

$$\lambda(k) = \lambda_0 \lambda(k-1) + (1-\lambda_0) \tag{5.16}$$

Here $\lambda(k)$ is considered to be a forgetting factor, reducing the identifiers responsiveness to early values of the error vector $z(k)-z(k)$. Figure 5-4 shows the improved convergence obtained with

$$\lambda_0 = 0.99 \tag{5.17}$$

and

$$\lambda(0) = 0.95 \tag{5.18}$$

when using $\gamma(k)$ as defined in Equation 5.15 to replace $\frac{1}{k^p}$ in Equation 5.8 . The smallest value of ξ_k has decreased below 5, but the improvement is not enough to produce an acceptable results in an acceptable observation time.

This slow convergence is predictable according to Ljung [Ref. 6:pp. 290-299]. It is suggested that the convergence rate can be improved with the Gauss-Newton algorithm. However, the Gauss-Newton algorithm has no advantage over the Kalman filter approach for the system being considered here.

E. SUMMARY

The stochastic gradient approach was chosen because it theoretically produces an unbiased estimate even in the presence of measurement noise. The simplicity of computation is a desirable feature. However, the computational simplicity of the steepest descent algorithm also means very slow convergence. The slow convergence of the algorithm could be improved with a more sophisticated choice of search direction. The improvement achieved by using an algorithm which is

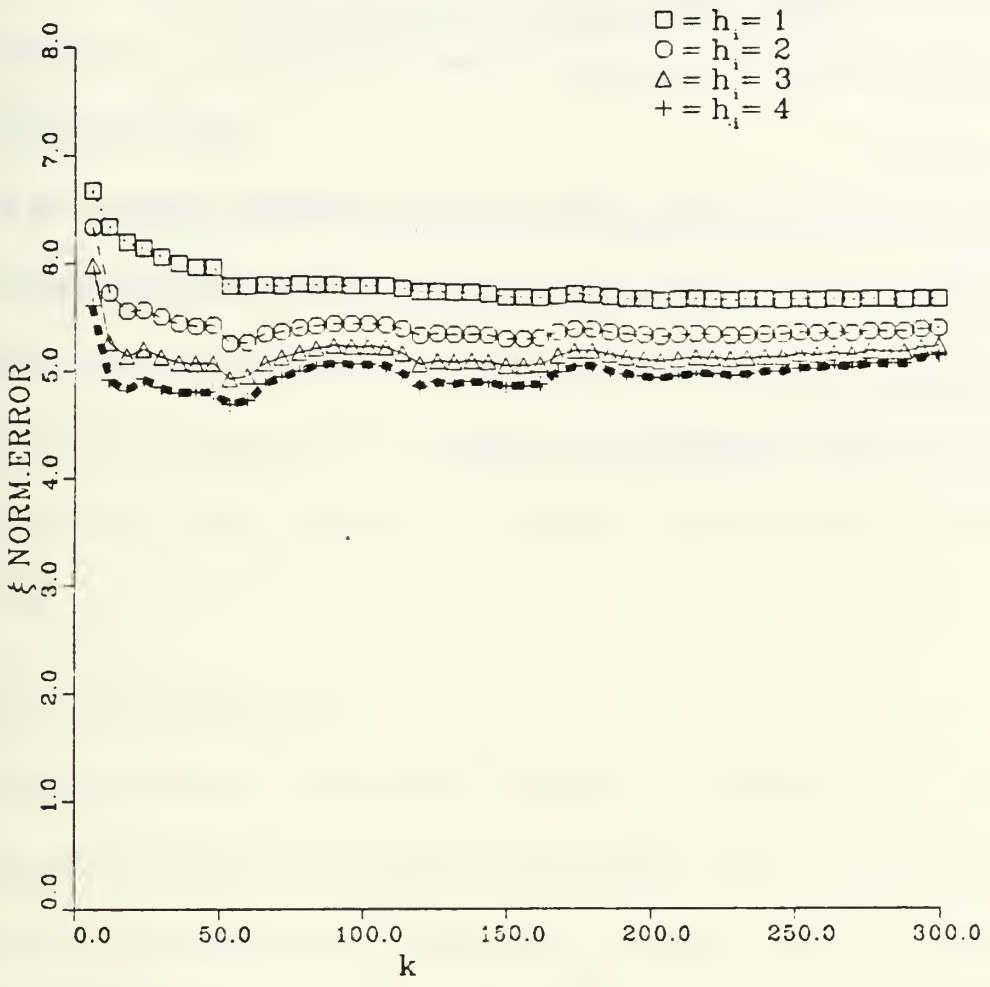

Figure 5-4 Parameter estimation error for four
different values of diagonal elements for Venters gain matrix.
and the use of a forgetting factor.
Initial conditions, $\sigma = 0.08$
Road noise, $\sigma = 0.1$
State measurement noise, $\sigma = 0.02$
State derivative measurement noise, $\sigma = 0.1$

correlated with $H(k)$ would be offset by the bias produced from this correlation. The use of the forgetting factor $\lambda(k)$ does improve the convergence, but this improvement is not significant enough to allow identification in an acceptable observation time.

Because of the slow convergence of the stochastic gradient approach, for the remainder of this thesis, it is abandoned in favor of the Kalman filter identifier. In the next chapter an improved model is introduced, which will introduce another facet of the land vehicle identification problem.

VI. IMPROVED MODEL IDENTIFICATION

A. INTRODUCTION

In the last three chapters a very simple vehicle model was used to test various identification algorithms. In this chapter a more realistic model is presented. The improved model is compared with the model developed in Chapter III, to determine how increased model size effects the identification process. Finally, the problem of two road noise inputs is discussed and the resulting identifier is analyzed.

B. AN IMPROVED MODEL

In Chapter III the simplified vehicle used for the simulation study of various identification schemes was developed. This simplified model has one very serious limitation that must be taken into account for an actual vehicle. The limitation is associated with the fact that it is a single input system, whereas an actual vehicle would have several inputs. Specifically, the inputs to the front and rear wheels will be correlated, and even if the white road noise approximation is considered valid, this correlation will produce a bias in an actual vehicle parameter identification. In order to analyze possible bias elimination schemes or in fact to determine if any approach is valid when there is correlation between the inputs, a

more realistic model is needed. In this section a eighth order, four-degree-of-freedom model is presented.

Consider the vehicle depicted in Figure 6-1. In this model the separation of the suspension into front and rear units, necessitates the introduction of rotational freedom about the lateral axis. This allows both rotational and vertical motion of the upper mass, the vehicle body.

The equations of motion for the improved vehicle are

$$\Sigma_{F_{x_1}} = -m_1\ddot{x}_1-[x_1-(x_3+\phi l_1)]k_{12} - [\dot{x}_1-(\dot{x}_3+\dot{\phi} l_1)]b_1 + (u_1(t)-x_1)k_{11} \tag{6.1}$$

$$\Sigma_{F_{x_2}} = -m_2\ddot{x}_2-[x_2-(x_3-\phi l_2)]k_{22} - [\dot{x}_2-(\dot{x}_3-\dot{\phi} l_2)]b_2 + (u_2(t)-x_2)k_{21} \tag{6.2}$$

$$\Sigma_{F_{x_3}} = -M\ddot{x}_3+[x_1-(x_3+\phi l_1)]k_{12}+[x_2-(x_3-\phi l_2)]k_{22} + [\dot{x}_1-\dot{x}_3+\dot{\phi} l_1)]b_1 + [\dot{x}_2-(\dot{x}_3-\dot{\phi} l_2)]b_2 \tag{6.3}$$

$$\Sigma_{M_\phi} = -J\ddot{\phi} + \{[x_1-(x_3+\phi l_1)]k_{12} + [\dot{x}_1-(\dot{x}_3+\phi l_1)]b_1\}l_1 - \{[x_2-(x_3-\phi l_2)]k_{22} + [\dot{x}_2-(\dot{x}_3-\dot{\phi} l_2)]b_2\}l_2 \tag{6.4}$$

where the equations have been linearized for small values of ϕ. The resulting state equations produce Equation 6.6, where the state vector is

$$x = \begin{bmatrix} x_1 \\ \dot{x}_1 \\ x_2 \\ \dot{x}_2 \\ x_3 \\ \dot{x}_3 \\ \phi \\ \dot{\phi} \end{bmatrix} \tag{6.5}$$

The upper mass M, is now supported by two wheels m_1 and m_2. The wheels

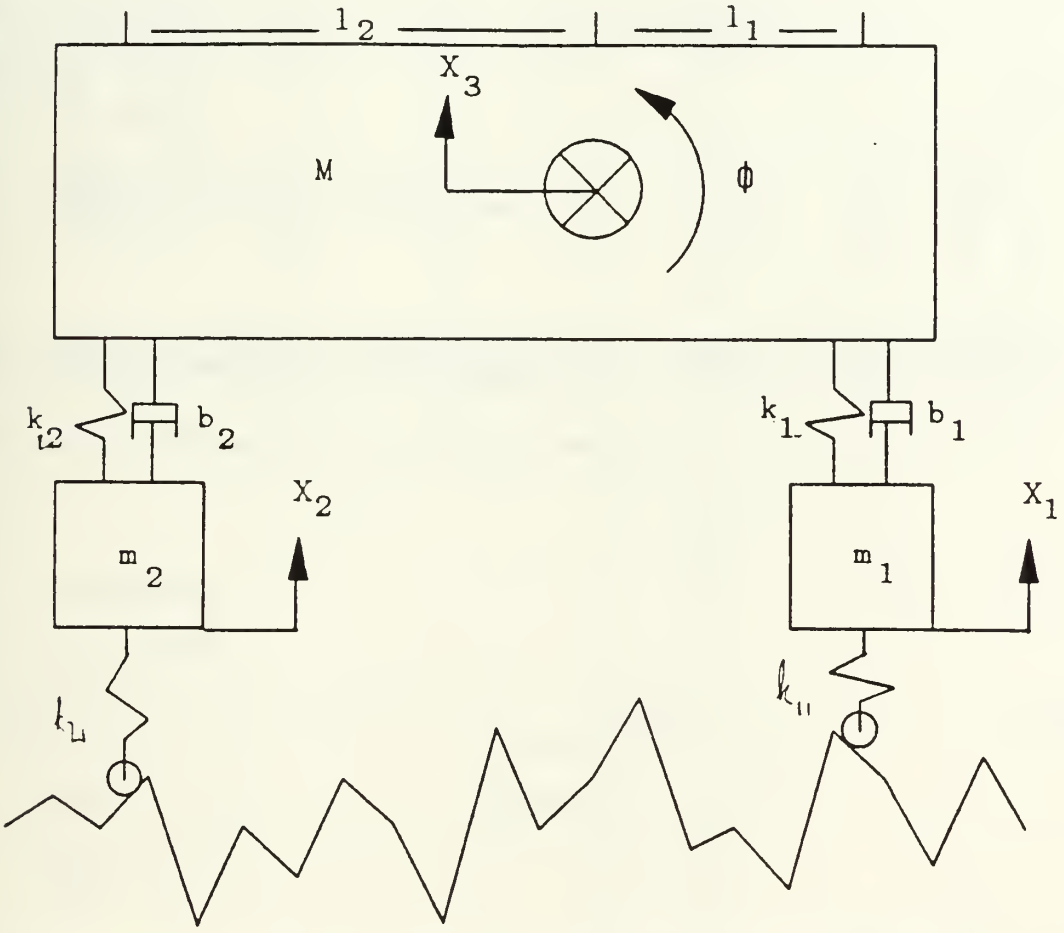

Figure 6-1 Improved Vehicle Model

$$\dot{x} = \tag{6.6}$$

$$\begin{pmatrix}
0 & 1 & 0 & 0 & 0 & 0 & 0 & 0 \\
\frac{-(k_{11}+k_{12})}{m_1} & \frac{-b_1}{m_1} & 0 & 0 & \frac{k_{12}}{m_1} & \frac{b_1}{m_1} & \frac{k_{12}l_1}{m_1} & \frac{b_1 l_1}{m_1} \\
0 & 0 & 0 & 1 & 0 & 0 & 0 & 0 \\
0 & 0 & \frac{-(k_{21}+k_{22})}{m_2} & \frac{-b_2}{m_2} & \frac{k_{22}}{m_2} & \frac{b_2}{m_2} & \frac{-k_{12}l_2}{m_2} & \frac{-b_2 l_2}{m_2} \\
0 & 0 & 0 & 0 & 0 & 1 & 0 & 0 \\
\frac{k_{12}}{M} & \frac{b_1}{M} & \frac{k_{22}}{M} & \frac{b_2}{M} & \frac{-(k_{12}+k_{22})}{M} & \frac{-(b_1+b_2)}{M} & \frac{l_1k_{12}-l_2k_{22}}{M} & \frac{b_1l_1-b_2l_2}{M} \\
0 & 0 & 0 & 0 & 0 & 0 & 0 & 1 \\
\frac{l_1k_{12}}{J} & \frac{l_1b_1}{J} & \frac{-l_2k_{22}}{J} & \frac{-l_2b_2}{J} & \frac{-l_2k_{22}+l_1k_{12}}{J} & \frac{-l_2b_2+l_1b_1}{J} & \frac{-l_1^2k_{12}-l_2^2k_{22}}{J} & \frac{-l_1^2b_1-l_2^2b_2}{J}
\end{pmatrix}$$

$$\times x + \begin{pmatrix}
0 & 0 \\
\frac{k_{11}}{m_1} & 0 \\
0 & 0 \\
0 & \frac{k_{21}}{m_2} \\
0 & 0 \\
0 & 0 \\
0 & 0 \\
0 & 0
\end{pmatrix} \begin{pmatrix} u(k) \\ u(k-\tau) \end{pmatrix}$$

are free to move vertically, while the body M, is free to move both vertically and to rotate about its center of mass, which need not be equidistant from the wheels. The angle of rotation ϕ, and the displacement x_3 describe the vehicle body, while x_1 pertains to the front wheel displacement and x_2 is the rear wheel displacement.

For the simulation study of this chapter the values selected for the dynamic components were

$$\begin{bmatrix} k_{11},\ k_{21} \\ k_{12},\ k_{22} \\ b_1,\ b_2 \\ m_1,\ m_2 \\ M \\ J \\ l_1 \\ l_2 \end{bmatrix} = \begin{bmatrix} 100 \\ 40 \\ 60 \\ 1 \\ 20 \\ 60 \\ 2 \\ 1 \end{bmatrix} \tag{6.7}$$

These values for the dynamic components of the system produce a vehicle model with roots of the characteristic equation located at

$$s = \begin{bmatrix} -.656 \pm j\ 3.11 \\ -.691 \pm j\ 2.08 \\ -.738 \\ -.837 \\ -61.5 \\ -65.3 \end{bmatrix} \tag{6.8}$$

As in the model developed in Chapter III, the input distribution matrix must be known, since the input vector is unknown, and the state vector x(k) and its derivative $\dot{x}(k)$ are measurable, but corrupted by noise.

In the improved model there are now two road noise inputs, which are correlated and shall be written as $u(k)$ and $u(k-\tau)$, where τ is the time delay between a road input to the front wheel and the same road input to the rear wheel. The value of τ is given in terms of the vehicle's velocity v, as

$$\tau = \frac{l}{v} \tag{6.9}$$

where l is the distance between the front and rear wheels. The correlation between $u(k)$ and $u(k-\tau)$ will be considered in detail in Section D. The other two noise sources remain the same, where $w(t)$ is the state measurement noise and $v(t)$ is the state derivative measurement noise.

In this chapter the parameter error measure ξ_k will be used again, with one minor change. The improved model parameters of Equation 6.5 have two zero values in each of the second and fourth rows. These zero values shall not be considered in the error measure ξ_k even though they appear in rows with unknown parameters. This assumption is a requirement of the definition of ξ_k given in Equation 3.17. This allows the use of the same error measure given by

$$\xi_k = \sum_{i=1}^{28} \left(\frac{\theta_i - \hat{\theta}_i(k)}{\theta_i} \right)^2 \tag{6.10}$$

The summation goes to 28 because the four zero values of rows 2 and 4 are not considered, and 32 of the 64 parameters are assumed known.

In the next section, the new model will be compared with the vehicle of Chapter IV to determine the effect increasing the state size has on system identification.

C. IMPROVED VEHICLE PARAMETER IDENTIFICATION

The opportunity to analyze the effect of changing state size on parameter identification should not be neglected, since only the sparsest reference is made to it in the literature. The change from a fourth order model to an eighth order model correspondingly changes the number of parameters from 16 to 64. As in the case of the fourth order system, half of the 64 parameter values are assumed known from the structure of the plant, and four more will not be considered in the parameter error measure ξ_k for the reasons discussed in the last section, leaving 28 parameters to be estimated. This rather substantial increase in parameters to be identified has a significant influence on the identification process. Making use of the results of Chapter IV, a comparison shall be made with the improved model under similar noise conditions. In this section the model will be excited using noise into the front suspension unit only. In the following section the improved model will be excited with road noise entering both suspension units and comparisons will be made.

1. P(0) Initialization

The initial value of the diagonal of P_0 plays an important role in the convergence rate of the Kalman filter identifier. Figure 6-2 shows how various values of the diagonal of P_0, the error covariance matrix, effect the identification process. Several observations can be made concerning the convergence rates as depicted by the parameter error measure ξ_k, especially when compared with the curves in Figure 4-1. The curve marked with "+" symbols produces the fastest

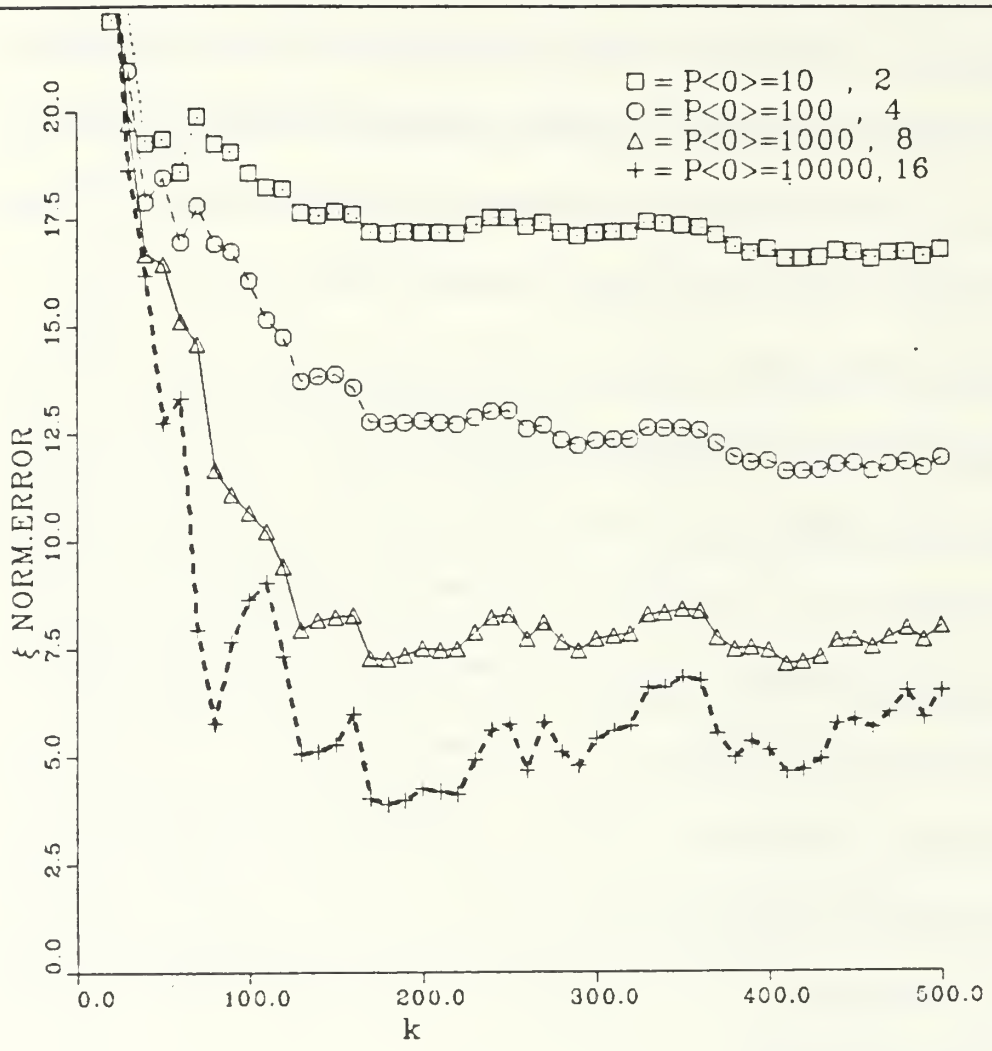

Figure 6-2 Parameter estimation error vs. number of iterations for four different initializations of the covariance matrix.
Initial conditions. σ =0.1
Road noise. σ =0.1
State measurement noise. σ =0.0
State derivative measurement noise. σ =0.005

initial convergence although the curve marked by triangles is approaching it and the triangled curve shows much better consistency during the early part of the identification. These remarks are true for both Figure 6-2 and 4-1. The higher order model must be broken into two diagonal blocks, because the size of the parameters in the sixth and eighth rows are so much smaller than the parameters of the second and fourth rows. Thus the second number in the legend is the value of the lower half diagonal of P(0). Because of its more consistent response. the value for the upper half diagonal of P_0 was chosen at 1000 and the lower half diagonal was selected at 8. The smaller value for the lower half diagonal of the P_0 matrix is due to the much smaller values of the elements of the sixth and eighth row parameters.

2. Convergence Rate of the Improved Model

The higher order of the improved model would lead to the assumption that convergence to acceptable parameter estimates will take longer than for the fourth order model. Figure 6-3 demonstrates the convergence rate for the eighth order model with only road noise excitation. Figure 4-2 shows the convergence rate for the fourth order model under the same noise conditions. It is difficult is compare convergence rates of systems of different order, but several observation can be made. In Figure 4-2, the plateauing effect is visible between 15,000 and 20,000 iteration. In higher order models the tendency for the parameter estimates to plateau is much greater and may require more iterations before improvement begins again. The plateauing effect in higher order models can be confused with a

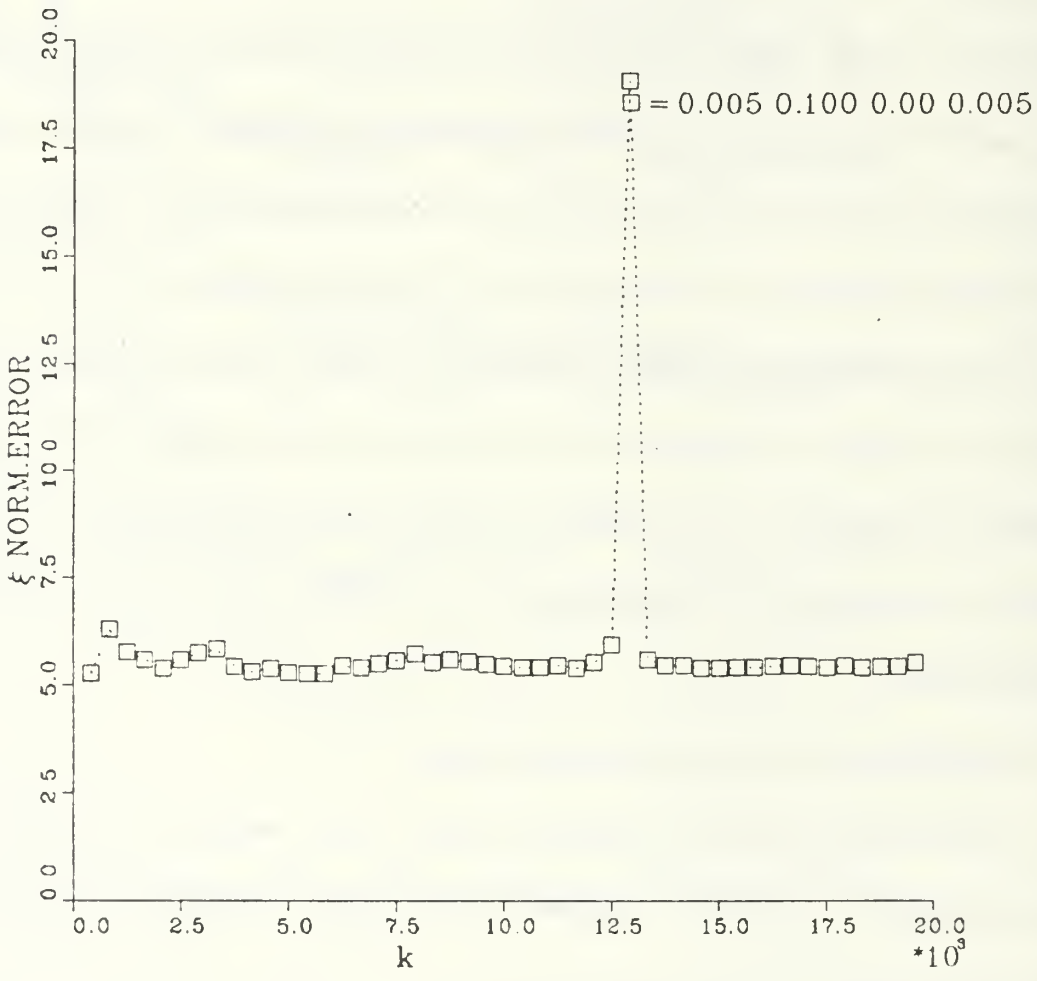

Figure 6-3 Parameter estimation error vs. number of iterations with road noise as the only system excitation.
Initial conditions, σ =0.0
Road noise, σ =0.1
State measurement noise, σ =0.0
State derivative measurement noise, σ =0.005

bias if one does not look carefully. The difference is that in the case of a bias the estimations will tend to become worse and there will be an increase in the estimation error measure ξ_k, while plateauing will result in essentially a flat error measure. In fact, during the simulation study of this eighth order model a plateau of 20,000 iterations was encountered. How to detect these long intervals with very little improvement in parameter estimation and what to do when a plateau is encountered is not addressed here. The fourth order model in Chapter IV required 40,000 iterations to identify the system parameters, while the eighth order model shows no improvement after 20,000 iterations for the same noise scenario. The parameter error measurement spike that occurs at approximately 13,000 iterations is somewhat mysterious. It seems likely, however, that it is caused by some form of system reflection where the input is reflected back from the rear wheel, appearing as a second input to which the identifier respond incorrectly.

3. Initial Conditions and Road Noise

Figure 6-4 illustrates the effect that large initial conditions and various amounts of road noise have on the Kalman filter identifier. Since only 6 of the 8 parameters in the second row are considered in the parameter error measure ξ_K, and there is road noise on only the second row estimates, the identifier is able to extract all of the other parameters except the second row. As the second row parameters are covered with road noise, little progress is made toward their

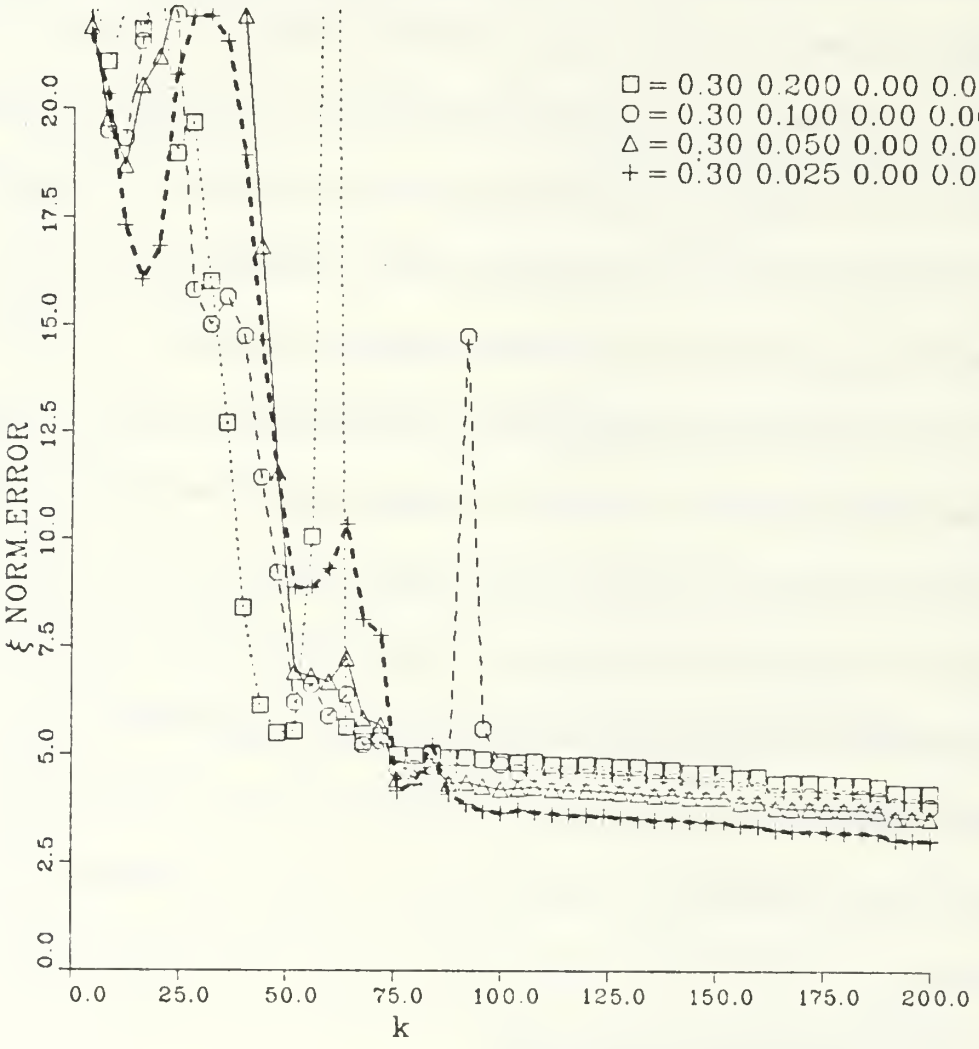

Figure 6-4 Parameter estimation error with various levels of road noise and constant initial conditions.
Initial conditions. σ =0.3
Road noise. σ =0.2. 0.1. 0.05. 0.025
State measurement noise. σ =0.0
State derivative measurement noise, σ =0.001

identification before the initial conditions diminish and the system's only excitation is from the road.

Comparing Figure 6-4 with Figure 4-3, some other observations can be made. Because of the larger search space of the eighth order system, it will usually require more iterations to reach acceptable identification. This can be seen in the slower convergence of Figure 6-4.

4. System Identification with Pulse Inputs

Figure 6-5 was produced using a P_0 matrix diagonally initialized with 1000. The increase in the estimators responsiveness is quite apparent. The curves in Figure 6-5 show the identification process when pulses of various widths are used. The curve marked by squares is the estimation error when the system is excited with an impulse, during the ninth measurement cycle. In the case of the fourth order system the energy absorbed by the system was enough to allow the identifier to estimate the parameters. In the eighth order model, because of the larger parameter inertia, the identifier is unable to reach acceptable identification before the impulse energy has dissipated.

5. Identification with State Measurement Noise

Figure 6-6 illustrates the tremendous effect state measurement noise has on the Kalman filter identifier when used in an eighth order system. The curve marked with "+" symbols has no state measurement noise, and the other three curves have varying levels of measurement noise. The system is excited by road noise. The curve marked with circles has measurement noise of only 1 % of the

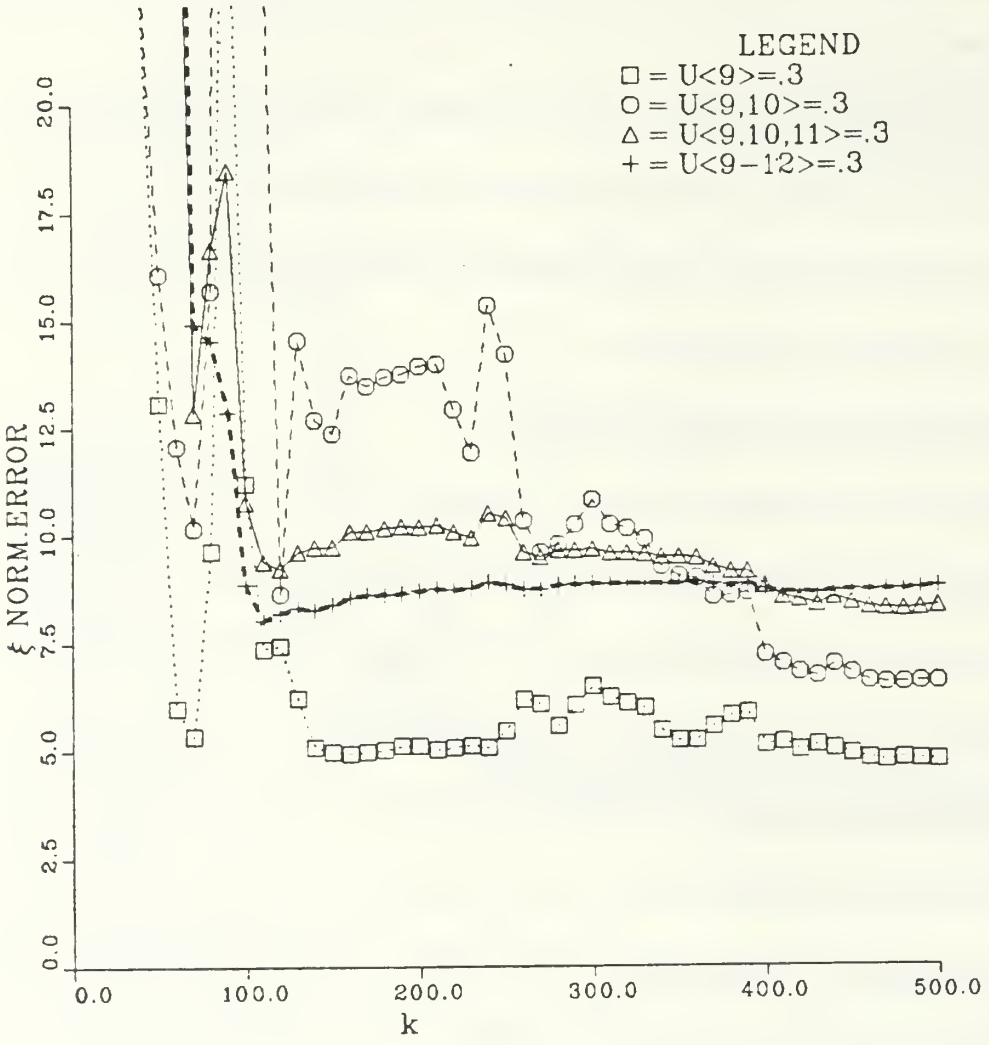

Figure 6-5 Parameter estimation error when system is excited with input pulses of various durations. Pulse duration shown in legend.
Initial conditions, σ =0.01
Road noise, σ =0.001
State measurement noise, σ =0.0
State derivative measurement noise, σ =0.01

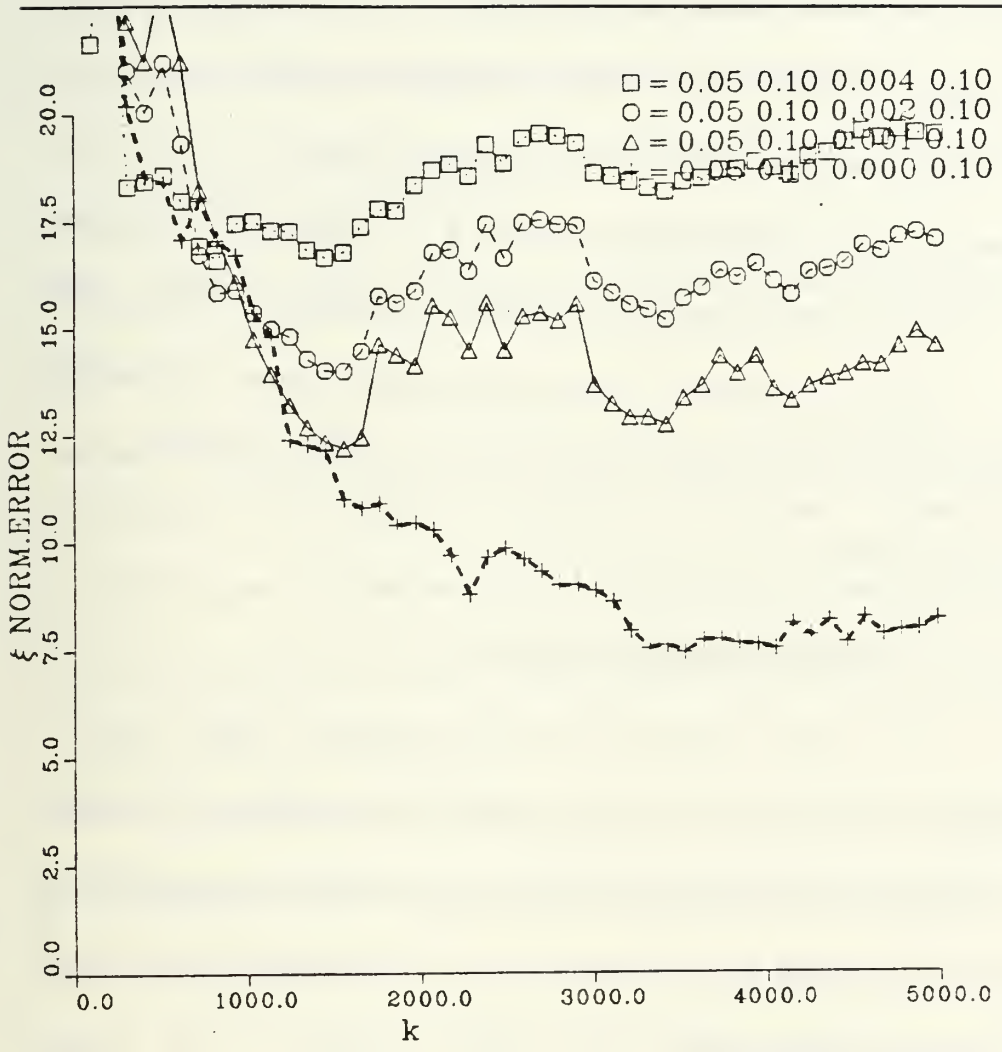

Figure 6-6 Parameter estimation error when various levels of measurement noise are added to the state vector.
Initial conditions, σ =0.05
Road noise, σ =0.1
State measurement noise, σ =0.002, 0.001, 0.0005, 0.0000
State derivative measurement noise, σ =0.1

road noise input to the system, and yet at 5000 iteration the parameter estimates are diverging. Figure 4-5 shows the identifiers estimation error for some of the same values of state measurement noise. In the simplified model, it can be seen that at 5000 iteration when measurement noise was 4 %, the identifier produced similar results. From this observation it is reasonable to assume that that eighth order model is 4 times as sensitive to state measurement noise and would therefore require sensors with a signal to noise ratio at least 6 dB greater than the fourth order model required.

D. TWO INPUTS TO THE IMPROVED MODEL

The use of a single road noise input into the improved vehicle model is somewhat artificial but does provide some insight into the effect of increased model size on the parameter identification process. The single input analysis of the last section also provides insight into results to be expected when two road noise inputs are applied to the model.

In this section the model will be excited with road noise through both wheels. The road noise into the front and rear suspension system of the vehicle will be correlated in time, since the front wheel will encounter an obstacle τ seconds before the rear wheel. Recall from Chapter IV Equation 4.11 that the bias on $\hat{\theta}(k)$ is the result of the input-output crosscorrelation as described in Equation 4.16. If the improved model is excited through the front wheel with an obstacle in the road, then the output, the state of the system will be correlated with the input to

the rear suspension when it encounters that same obstacle τ seconds later. Then from Equation 4.11, the bias produced by this correlation will be

$$[P^{-1}(0) + P^{-1}(k)]^{-1} \sum_{m=1}^{k} H^T(m) R^{-1} v(m) \qquad (6.11)$$

where v(m) is the total noise vector including $u(k-\tau)$, which is correlated with $H^T(m)$.

A possible solution to the input-output crosscorrelation bias that will undoubtedly result in slower convergence is as follows. Assume for a moment that the parameters of the second row of Equation 6.5 are known exactly. This being true, then the first element of the error vector is defined by

$$e_1(k) = z_2 - \mathrm{x}\theta_{1-8} = v_2(k) + b_{21}u(k) \qquad (6.12)$$

where θ_{1-8} represents the first 8 elements of the $\hat{\theta}$ vector, which are known exactly. The discrepancy in the subscripts resides in the fact the the first and third rows of the A matrix are assumed known and therefore are not part of the identification process. If it is further assumed that the measurement noise is negligible compared to the road noise, then

$$b_{21}u(k) \approx e_1(k) \qquad (6.13)$$

In order to eliminate the effect of the road noise from the identifier, the measurement samples must be taken when the rear wheel is exactly over the same position on the road that was samples τ iterations before when the front wheel was over that point. This can be accomplished because of the asynchronous nature of the identification scheme presented here. If this element of the error vector is

then subtracted from the second element of the error vector τ seconds later, this will eliminate the road noise from the error vector and the identifier will produce an unbiased estimate. This can be expressed mathematically as

$$e_2(k) = z_4 - x\hat{\theta}_{9-16} - e_1(k-\tau) = v_4(k) + g(x(k), \theta_{9-16}, \hat{\theta}_{9-16}) + b_{42}u(k) - b_{21}u(k-\tau) - v_2(k-\tau) \quad (6.14)$$

where the two input term on the right side of the equation cancel. The assumptions used earlier may now be lifted since $e_1(k-\tau)$ is white noise. This can be seen if Equation 6.12 is considered as a whitening filter. Then $e_1(k-\tau)$ is an innovation sequence and it can be shown that [Ref. 7:p. 250]

$$E[e_1(k-\tau) \mid z_2(k-\tau-1), \ldots, z_2(k_0)] = 0 \quad (6.15)$$

The convergence rate of this approach will certainly be affected, since the variance of the noise on the fourth row parameters is very large until the parameter estimates of the second row of Equation 6.5 become more accurate.

Before analyzing the bias elimination scheme proposed above, a look will be taken at how the identifier responds to two independent road noise inputs and then the bias itself will be shown. Figure 6-7 illustrates the parameter error when two different road noise ensembles are input to the front and rear suspension units of the improved model. As one might have anticipated, the added noise source results in less effective identification of the fourth row parameters which translates into higher values of the parameter error measure. However, the identification is somewhat better than one might expect. When two different road noise inputs are applied to the vehicle the resulting parameter error is not twice as bad as when a single input is applied. The plateau is again present for the last 4000 iterations.

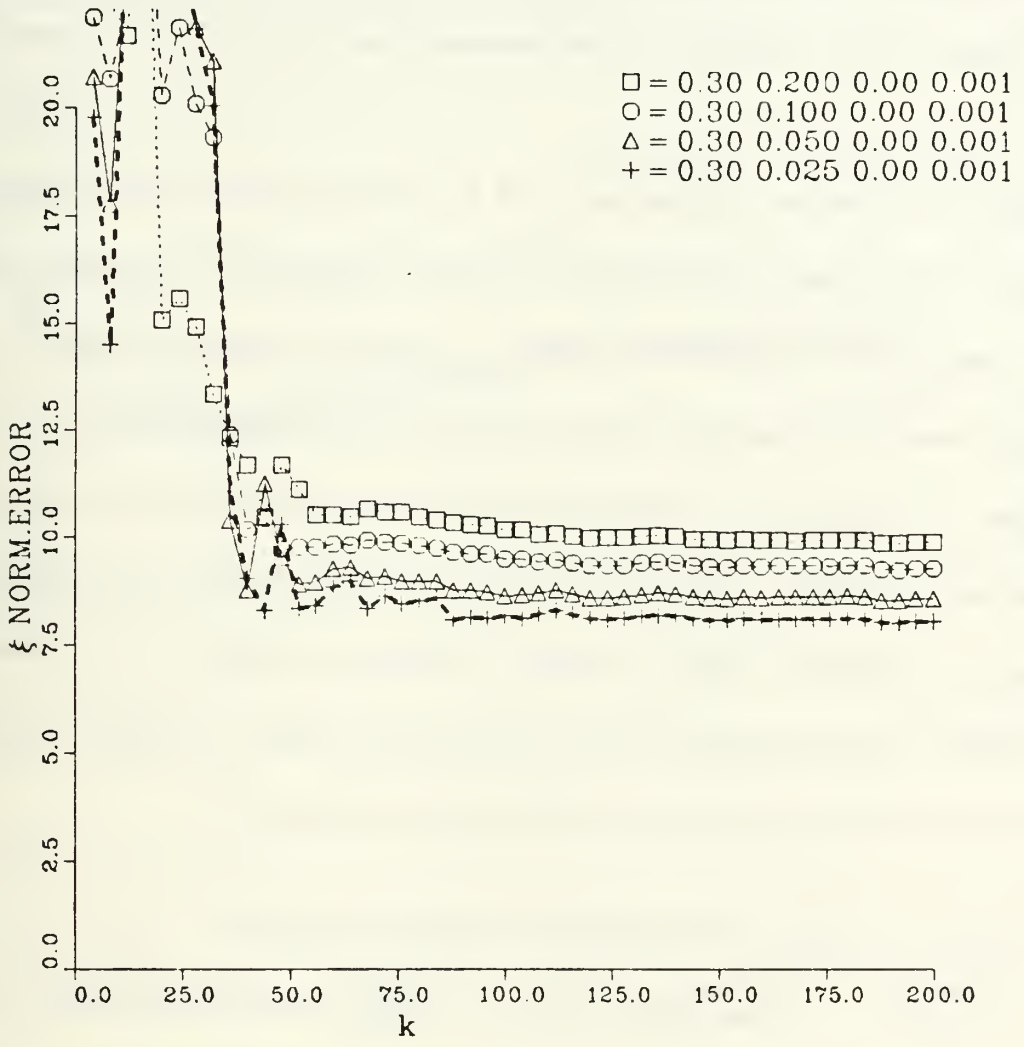

Figure 6-7 Parameter estimation error vs. number of iterations for four different values of road noise, holding initial conditions constant, for two independent noise inputs.
Initial conditions, σ =0.3
Road noise, σ =0.2, 0.1, 0.05, 0.025
State measurement noise, σ =0.0
State derivative measurement noise, σ =0.001

One other observation concerning Figure 6-7 is that the plateaus appear to be quite distinct. There is a plateau at the parameter error value of 9 and another at 7.5.

When two correlated inputs are used to excite the vehicle the resulting parameter error measure is biased. This is shown in Figure 6-8. Notice that after 1000 iterations the identification process is producing estimates which are becoming worse. This bias is the result of the input-output crosscorrelation.

Figure 6-9 illustrates the improved identifier performance when the the bias elimination developed in Equations 6.12-6.14 are incorporated in the parameter estimation algorithm. Using the bias elimination scheme, the parameter measurement error approaches that of a single input shown in Figure 6-3. This curve was made by setting P_0 equal to 1000 along the diagonal.

E. COMPUTATIONAL AND STORAGE REQUIREMENTS

In Chapter IV it was found that the computational requirements of the algorithm were within the capability of a microprocessor. This is not the case for the eighth order system analyzed in this chapter. Also, since the parameters of the fourth, sixth and eighth rows are less corrupted by noise, the algorithm could stop searching for those parameters long before the parameters of the second row are found. This capability can be accomplished by using the structure of this identification approach. Recall that Equation 2.3, constructs the $H(k)$ matrix by

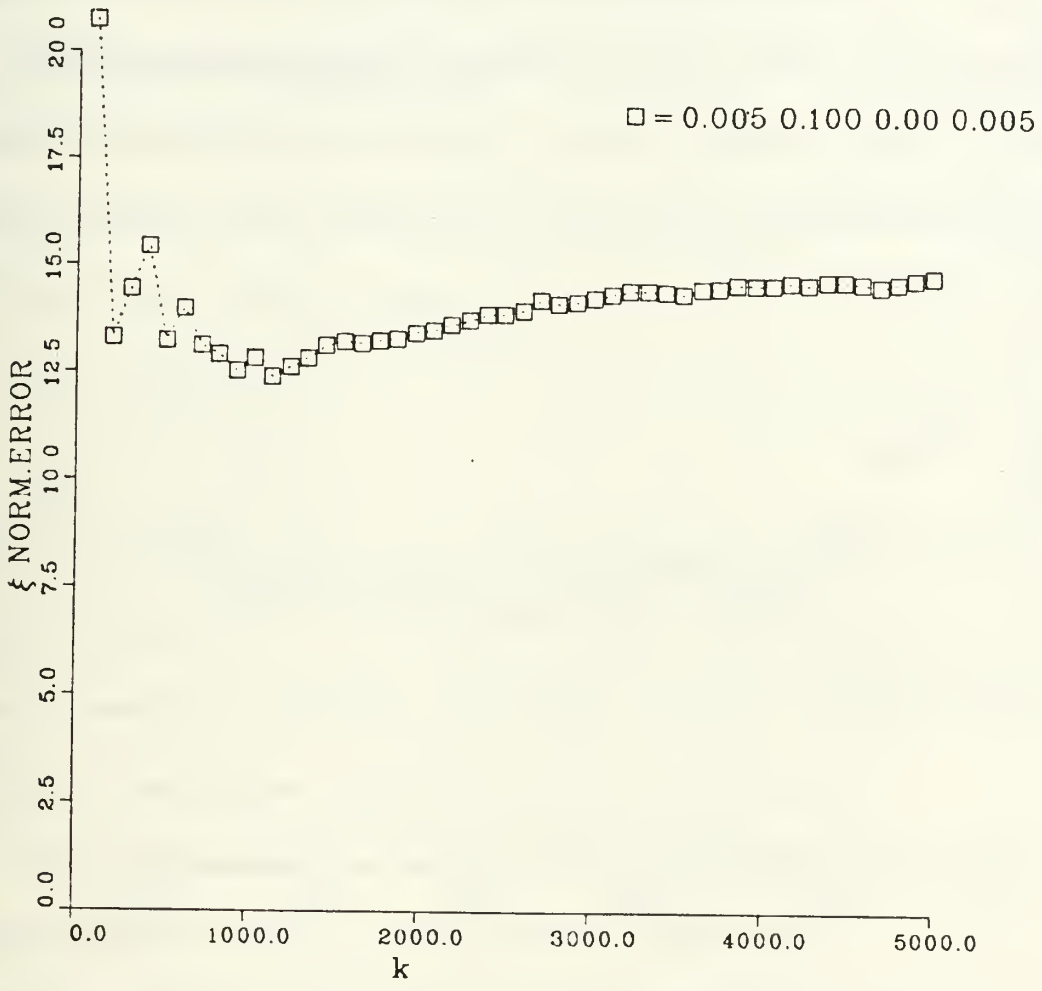

Figure 6-8 Parameter estimation error vs. number of iterations with correlated road noise as the only form of excitation.
Initial conditions, σ =0.0
Road noise, σ =0.1
State measurement noise, σ =0.0
State derivative measurement noise, σ =0.005

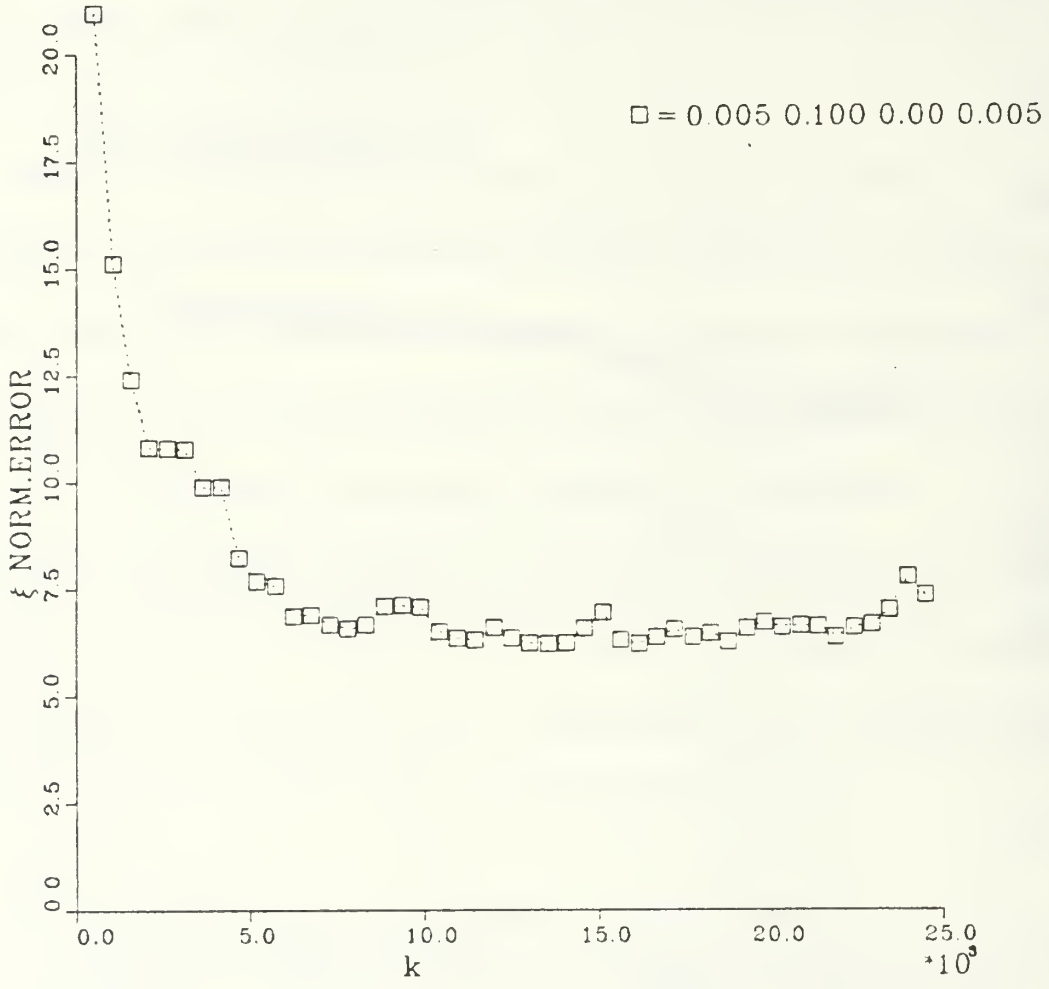

Figure 6-9 Parameter estimation error vs. number of iterations with correlated road noise as the only form of excitation and bias elimination is used.
Initial conditions. σ =0.0
Road noise. σ =0.1
State measurement noise. σ =0.0
State derivative measurement noise. σ =0.005

using disjoint state vectors. Thus, the identifier may be considered as four separate identifiers, which are associated by the state vector alone.

This allows the algorithm to be broken into four separate scalar identifiers, which eliminates the need to perform a matrix inversion. If each of the new, smaller parameter vectors is denoted by θ', then the new algorithm is given by

$$\theta'(k) = \theta'(k-1) + g'(k)[z_i(k) - x^T\theta'(k-1)] \tag{6.16}$$

$$g'(k) = \frac{P'(k-1)x}{x^T P'(k-1)x + r_i} \tag{6.17}$$

$$P'(k) = [\, I - g'(k)x^T]P'(k-1) \tag{6.18}$$

where $g'(k)$ is now the gain vector. The separation of the parameter vector will require this algorithm to be performed four times during each iteration, but as a row of parameters is identified it can be eliminated from the algorithm. This will reduce the computational requirements and thus the cycle time.

Each time through the algorithm the microprocessor will perform 270 multiplications, 8 divisions, 255 additions, 344 index register increments, 277 loads, and 96 stores. Using the same operation times as in Chapter IV, the total time required per shortened parameter vector is 3628 μseconds. Therefore, one iteration requires 14,512 μseconds or 0.0145 seconds. The asynchronous algorithm developed in this thesis does not depend on the time interval between measurements. This will allow the algorithm to reduce the interval between measurements as parameter rows are identified and dropped from the algorithm. The memory requirement is 2800 bytes for all four algorithms.

F. SUMMARY

Parameter identification in high order systems is fraught with peril. As the number of parameters to be identified increases, so does the dimension of the search space. This increase in the search volume results in plateauing. When the noise added to the state derivative is large as in the case of road noise, then these plateaus become very expansive, and it is not clear that identification is even possible. However, in most applications the parameters of the body are probably more important than those of the wheels.

The observant reader might have noticed that in none of the parameter estimation error curve of this chapter, did the error reduce below about 5. In fact, on several simulations not shown, the error did reach acceptable values. These low errors were obtained when the initial conditions were very large and the noise added to the measurements was very small.

VII. SUMMARY AND CONCLUSIONS

A. INTRODUCTION

In the previous six chapters, the theoretical results of parameter identification were presented, and applied to the problem of estimating the dynamic parameters of a land vehicle. The simulation studies performed in the last four chapters demonstrated the capabilities of each approach. In this chapter an overview of the result is given, and suggestions for further study presented.

B. RESULTS

The batch-process least squares procedure of Chapter III was judged to be impractical because it required the storage of all the data before the identification process could begin. The recursive form of this algorithm is the Kalman filter identifier without the theoretical insight of how to choose P(0).

The identification of the dynamic parameters of a land vehicle is possible with the Kalman filter identifier. The practicality of this approach is in question, however. There are several practical drawbacks to the identification scheme presented here that make it extremely costly to implement. Most autonomous vehicles have an inertial navigation system on board, thus the elements of the state vector dealing with the vehicle bodies position, velocity, acceleration, and their angular counterparts are available. These measurements will probably be

quite accurate and have reasonable signal to noise ratios. The wheel positions, velocities and accelerations are another matter. It is not likely that an accelerometer would be mounted on each wheel to measure its acceleration. Each wheel's acceleration could then be integrated to obtain its velocity, which in turn could be integrated to find the wheel's position. It might be possible to find the acceleration on each wheel with respect to the body with a less sophisticated device than an accelerometer, which could then be added to the vehicle's acceleration to find the inertial space acceleration on the wheel. In either case, there is a requirement to develop the states of each wheel. On vehicle with several wheels (more than four) this will become quite hardware intensive.

The stochastic gradient identifier using the steepest descent algorithm was extremely susceptible to plateauing. The Lyapunov gain matrix produced better results, but the R(k) matrix was correlated with the H(k) matrix which would necessarily produce a bias. The extent of this bias was not analyzed.

The problem of plateauing observed in the last chapter, is unresolved. Plateauing is quite common in least squares identification, or the Kalman filter approach. This problem was also seen in the stochastic gradient algorithm to a much worse degree. The algorithm did obtain acceptable estimates for the parameters that were not corrupted by road noise. In the case of correlated inputs, the scheme was able to identify the rear wheel parameters. If the center of gravity of the vehicle is known, and the dynamic elements of the front and rear wheels are the same, it should be possible to obtain the front wheel parameters

from the rear wheel elements. In order to remove the correlate between the inputs to the front and rear wheels. it was necessary to allow the time interval between samples to vary. This variation in sampling interval allowed the system to take measurements when when the rear wheel is over a point where a front wheel measurement was taken. The problem of state measurement noise bias worsened with the increase in state size. This is not surprising, but presents a severe limitation to this form of identification. Two possible solutions to be investigated are presented in the next section.

The scheme used to remove the correlation between the input and the state was successful. The implementation of this scheme might prove difficult. Whenever there is a requirement for an object to be over exactly one location at the proper time there is not much room for error. The question of exactly how accurate this timing must be. to obtain acceptable results. might best be answered on a real vehicle.

The Kalman filter identifier possessed the best characteristic of the three identification schemes chosen for analysis in this thesis, but it has a very limited capability to perform in the scenario described in Chapter I. Under different conditions it might perform much better. If for instance. several of the vehicles dynamic elements were known. but some others were likely to change very slowly throughout their operating life time. the number of parameters to be identified would decrease. This decrease would allow the Kalman filter to function more effectively.

The least squares approach works very well when there are large initial conditions, even in the presence of substantial measurement noise. The Kalman filter identifier, being a recursive least squares algorithm, should perform as well with the proper initial conditions. Thus, if the identifier is activated after large initial conditions have been imparted to the vehicle, it should produce much better results. This procedure would improve both the plateauing problem and the state measurement noise bias.

C. FURTHER STUDY

This thesis dealt with a methodology and did not attempt to use the parameters of an actual vehicle or the limitations of actual measurement equipment. Before any experimentation is done on an actual vehicle with real measurement equipment, several aspects of the work done in this thesis deserve further investigation.

The present analysis shows that the signal to noise ratio of the vehicle state sensors must be approximately 40 dB. This is an rather large signal to noise ratio for this type of sensor. There are two possible solution to this problem which should be investigated. The first is the extended Kalman filter identifier [Ref. 6:pp. 422-23]. Theoretically this approach estimates the state and identifies the parameters. There are no perpetual motion machines, however, and the price for this more complicated identifier will certainly be slower convergence. If on the

other hand, the slower convergence is not excessive, this approach would then be an excellent prospect for a vehicle identifier.

The other possible solution deals with the stochastic gradient approach. This approach was unsuccessful using the Venter gain matrix, and the Lyapunov gain matrix approach was abandoned because of theoretical inconsistencies. The resulting effect of this inconsistency was not investigated. This approach may perform somewhat better than the Kalman filter, even though theoretically flawed, when moderate state measurement noise is present.

The investigation of parameter tracking was not completed in this thesis. Although this area of analysis is easily interpolated from the previous study, no real experimentation was done. Therefore, the study of the parameter tracking problem, and which approach to use remains to be completed.

In chapter VI, the problem of plateauing was identified, but no analysis was done to try to reduce the probability of its occurrence. The use of a reinitialization scheme, such as the one discussed in Chapter IV, may allow the identifier to break through plateaus. This would reduce this serious problem to one of identification of plateaus, and decisions on how wide a plateau must be before reinitialization is preformed.

LIST OF REFERENCES

1. Adam, J. A., "Technology '86: Aerospace and Military," IEEE Spectrum, pp. 76-81, January 1986.

2. Nitao, J. J. and Parodi, A. M., "A Real-Time Reflexive Pilot for an Autonomous Land Vehicle," IEEE Control Systems, pp.14-23, February 1986.

3. Horgan, J., "Roboticists Aim to Ape Nature," IEEE Spectrum, pp. 66-71, February 1986.

4. Mendel, J. M., **Discrete Techniques of Parameter Estimation: The Equation Error Formulation**, Mercel Dekker, Inc., 1973.

5. Gelb, A., **Optimal Estimation**, The M.I.T. Press, 1974.

6. Ljung, L. and Soderstrom, T., **Theory and Practice of Recursive Identification**, The M.I.T. Press, 1986.

7. Goodwin, G. C. and Sin, K. S., **Adaptive Filtering Prediction and Control**, Prentice-Hall, Inc., 1984.

8. Cooper, G. R. and McGillem, C. D., **Probabilistic Methods of Signal and System Analysis**, Holt, Rinehart and Winston, Inc., 1971.

INITIAL DISTRIBUTION LIST

		No. Copies
1.	Library, Code 0142 Naval Postgraduate School Monterey, California 93943-5002	2
2.	Chairman, Code 62 Department of Electrical and Computer Engineering Naval Postgraduate School Monterey, California 93943-5000	1
3.	Prof. Robert B. McGhee, Code 52MZ Department of Computer Science Naval Postgraduate School Monterey, California 93943-5000	1
4.	Prof. Srbijanka Turajlic, Code 62TC Department of Electrical and Computer Engineering Naval Postgraduate School Monterey, California 93943-5000	1
5.	Prof. Roberto Cristi, Code 62CX Department of Electrical and Computer Engineering Naval Postgraduate School Monterey, California 93943-5000	1
6.	Prof. Harold Titus, Code 62TS Department of Electrical and Computer Engineering Naval Postgraduate School Monterey, California 93943-5000	1
7.	Mr. Scott Harmon, Code 442 Naval Ocean Systems Center San Diego, California 92152	1
8.	Dr. Andrew Chang FMC Corporation Central Engineering Laboratories Santa Clara, California 95092	1

9.	Dr. James W. Lowrie Martin Marietta Denver Aerospace P.O. Box 179 Denver, Colorado 80201	1
10.	Dr. William Isler Defense Advanced Research Projects Agency 1400 Wilson Blvd. Arlington, Va 22209	1
11.	Defense Technical Information Center Cameron Station Alexandria, Virginia 22304-6145	2
12.	Capt. James Kessler 13287 Kitten Ct. Woodbridge, Virginia 22193	1

17898 2

DUDLEY KNOX LIBRARY
NAVAL POSTGRADUATE SCHOOL
MONTEREY, CALIFORNIA 93943-5002

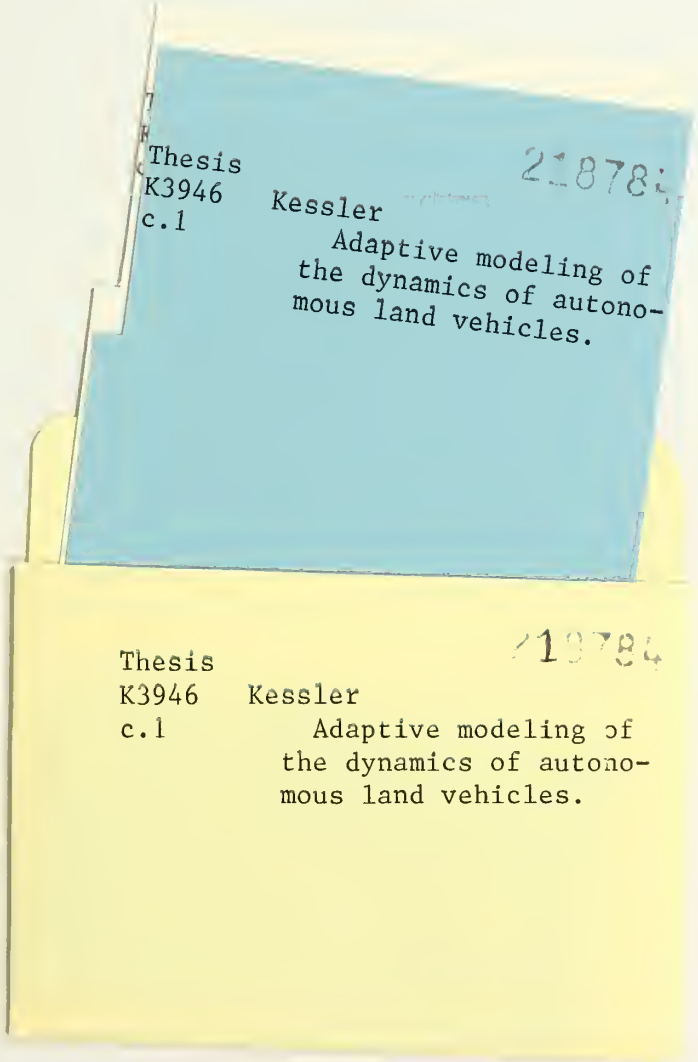

thesis3940
Adaptive modeling of the dynamics of aut
3 2768 000 67083 0
DUDLEY KNOX LIBRARY